HF and ELF facilities as the educational tools for Geospace research

A.V. Koloskov , Y.M. Yampolsky, C. La Hoz, S.B. Kascheev, A.S. Kascheev, I.I.Pikulik

Institute of Radio Astronomy of NASU, 4, Chervonoprapotna Str, Kharkiv, 61002, Ukraine

UiT The Arcric University of Norway, Tromsø NO-9037, Norway

HF facility

- High accuracy Doppler shift measurements (long-term stability ~ 10 ppb per day)
- High sensitivity and performance
- Fully automated and remotely controlled
- Low-cost, software-defined, mounted inside standard PC

Reference signal source

HF Doppler receiver (Winradio G313i) up to 3 units in one PC

Active loop antenna

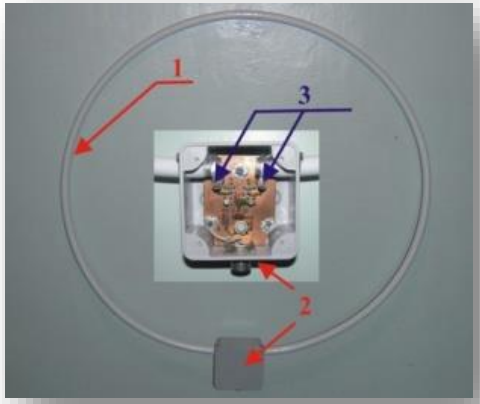

- Frequency Band 3-30 MHz
- Receiver bandwidth 0.5-22 kHz
- Tuning accuracy 1 Hz

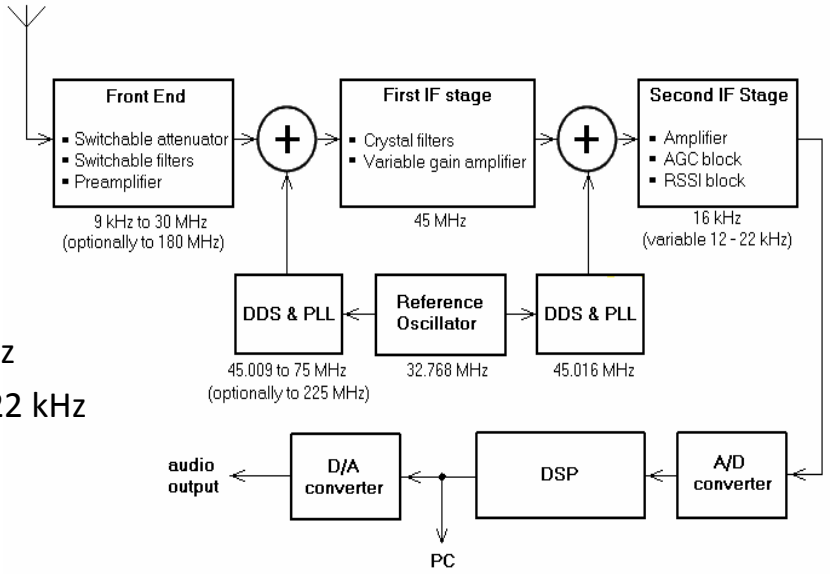

Location

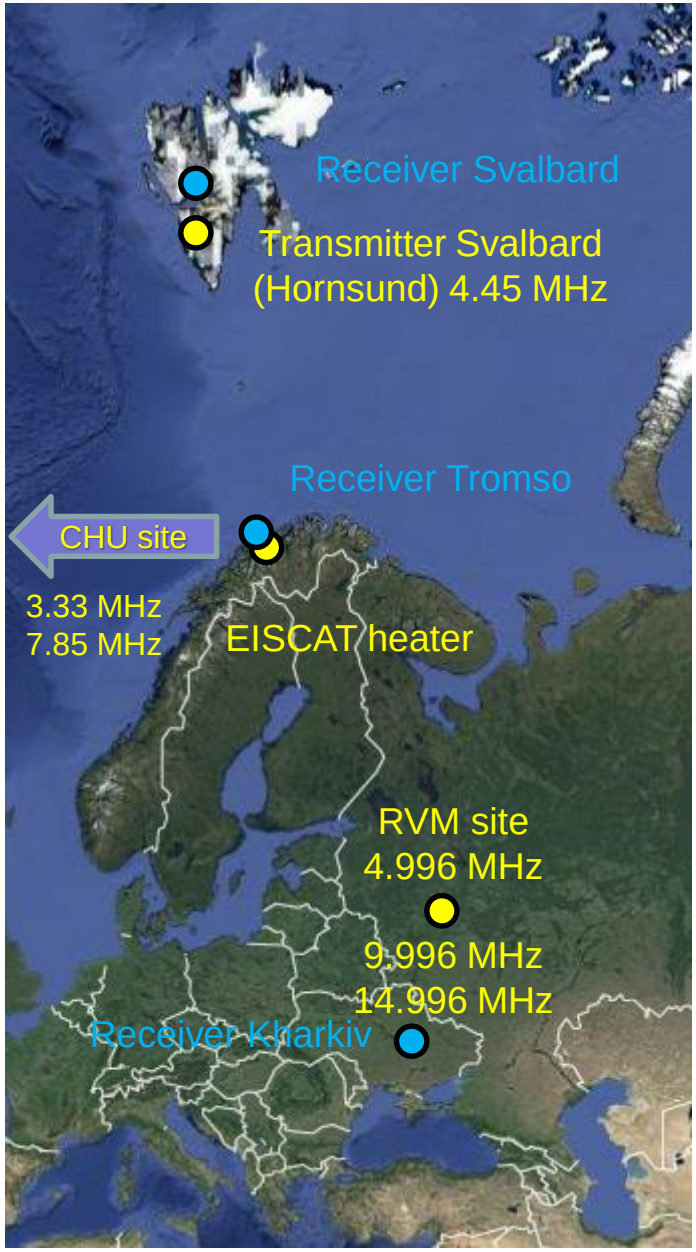

Tromso

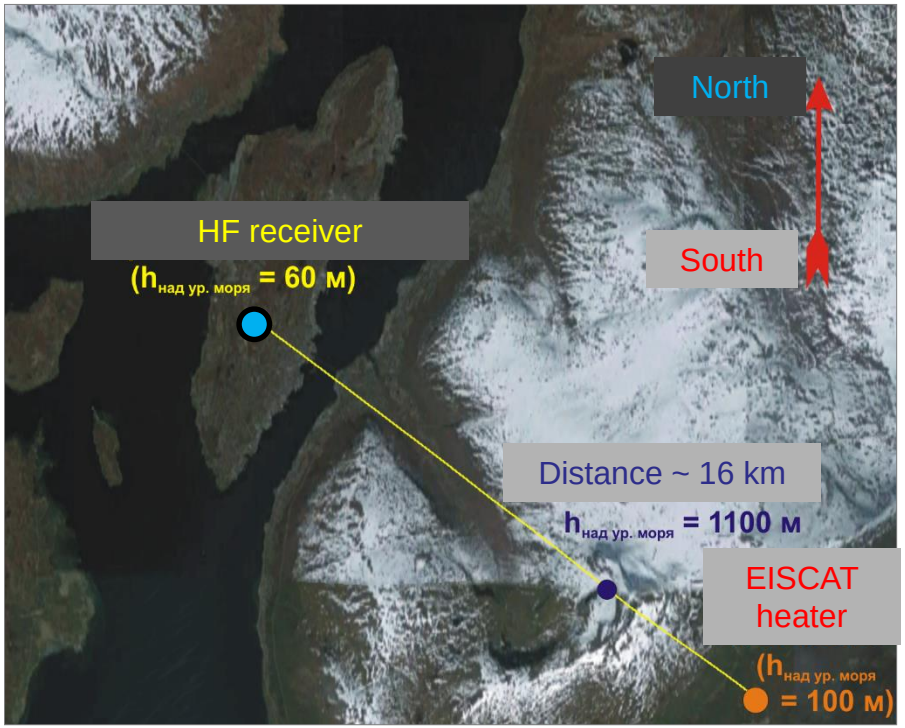

Network of the HF receivers

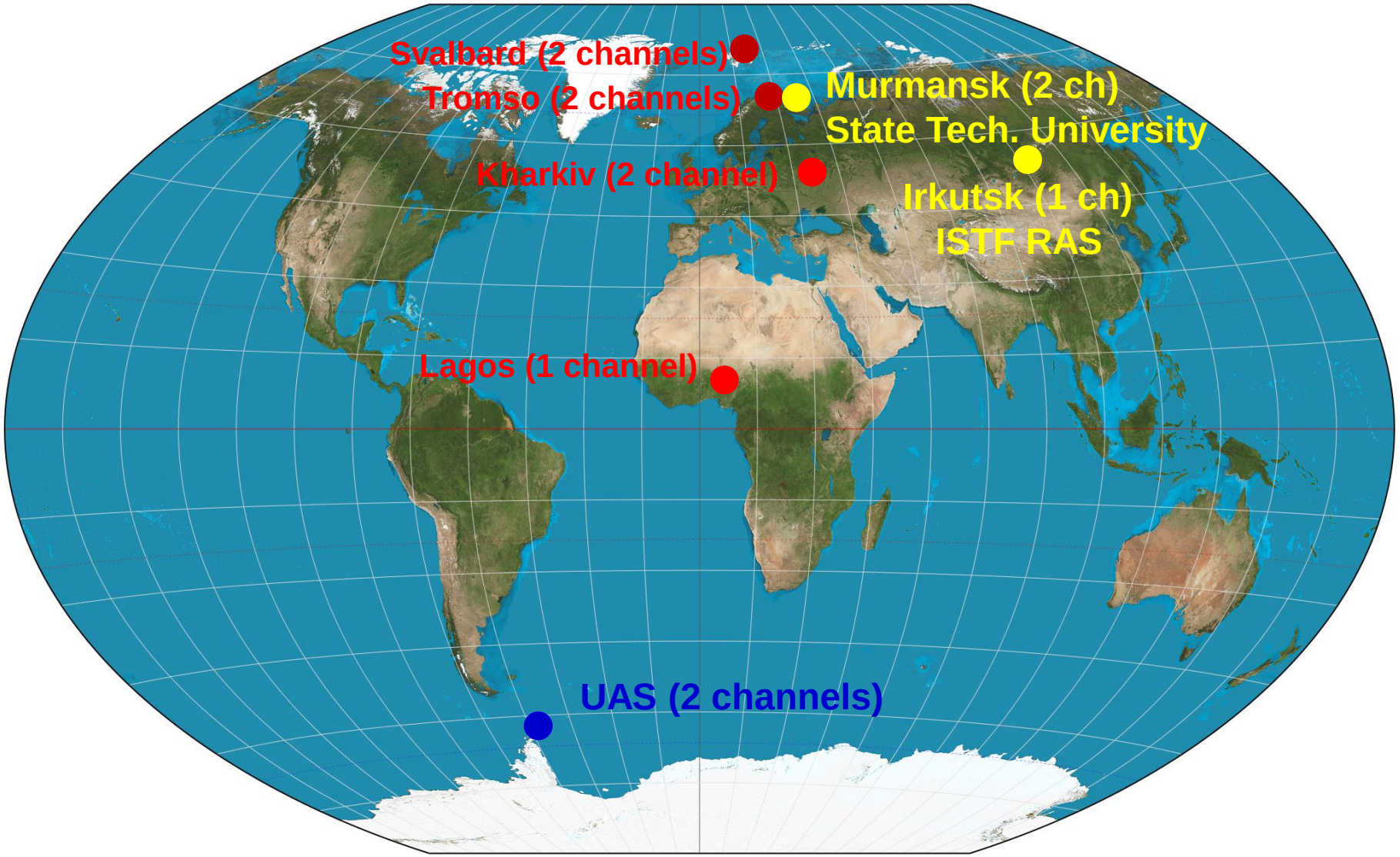

Internet-controlled Manually-controlled Partner instruments

ELF facility at Svalbard

Lemi-112E	
Frequency band (wide)	0.001 - 80 Hz
Sampling rate	254 Hz
Magnetic noise level at 0.001 Hz Magnetic noise level at 0.01 Hz Magnetic noise level at 1 Hz Magnetic noise level at 10 Hz	< 200 pT/√Hz < 20 pT/√Hz < 0.2 pT/√Hz < 0.03 pT/√Hz

ELF sensor

ELF facility near Kharkiv

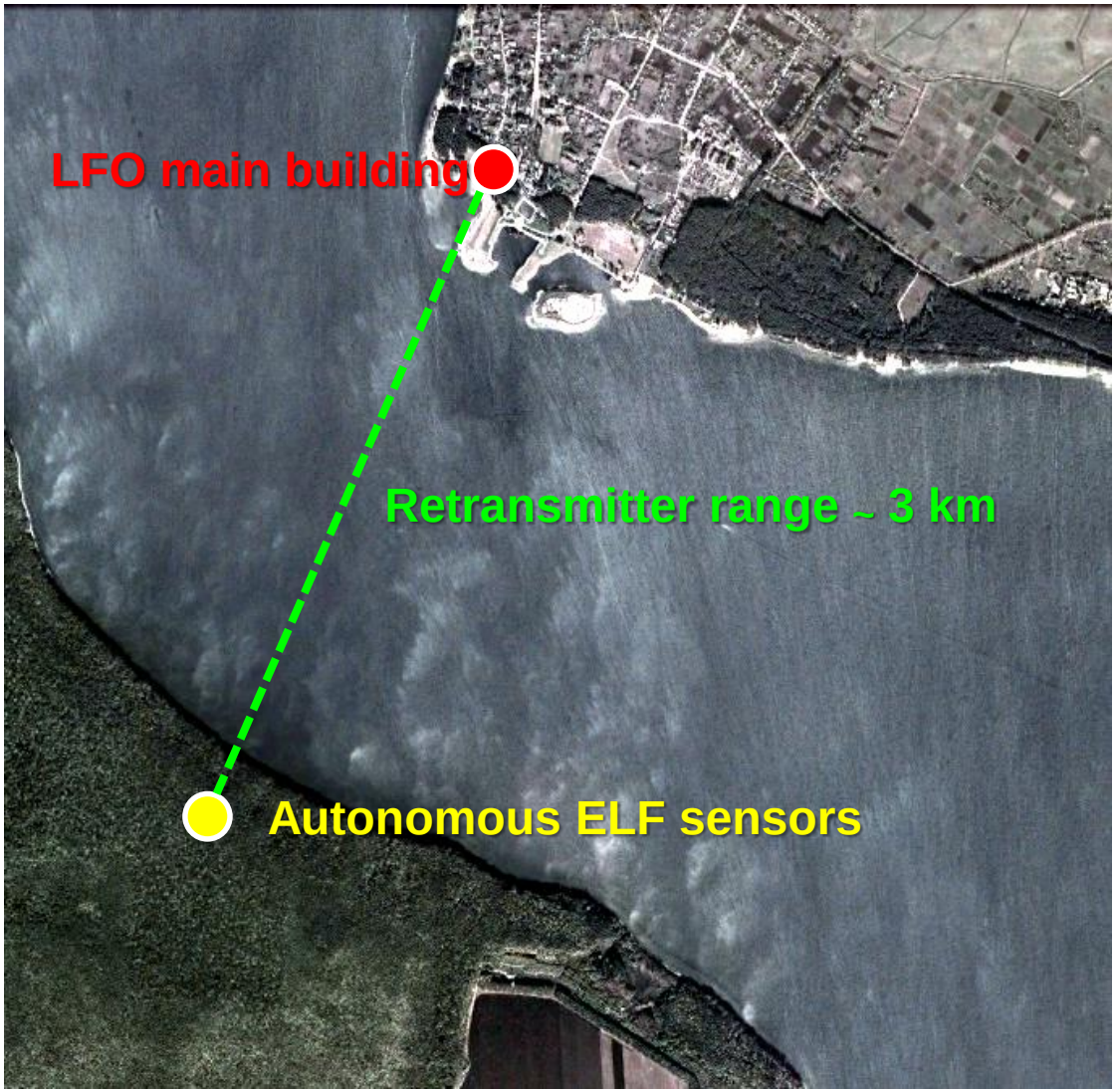

Frequency range	0.5 - 40 Hz
Sampling rate	125 Hz
Retransmitter frequency	433 MHz
Retransmitter power	1 mW
Retransmitter range	≈ 3 km

Network of the ELF magnetometers

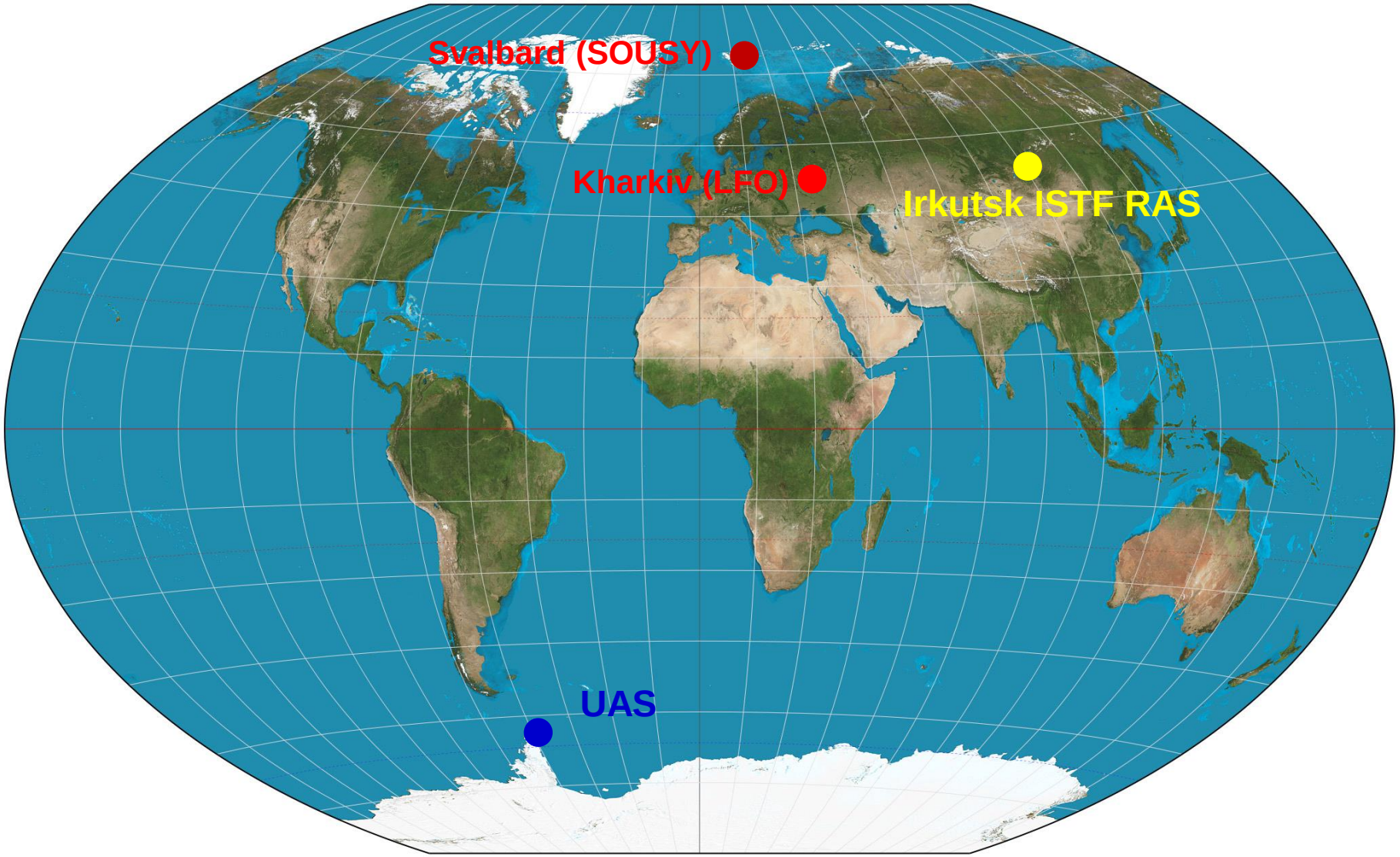

Remote control and real-time Internet access to data, data visualizing

IRA and UiT workstations

IRA Server, Ukraine

Internet

KHO, Svalbard (HF)

Tromso, Norway (HF)

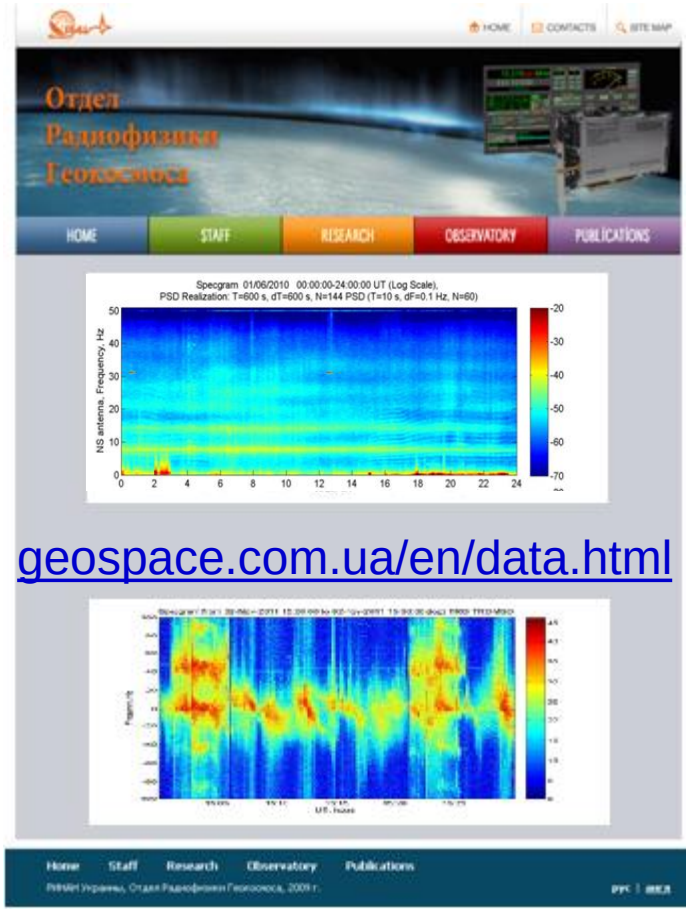

geospace.com.ua/en/data.html

LFO, Ukraine (HF, ELF)

SOUSY, Svalbard (ELF)

Layout of the HF observations

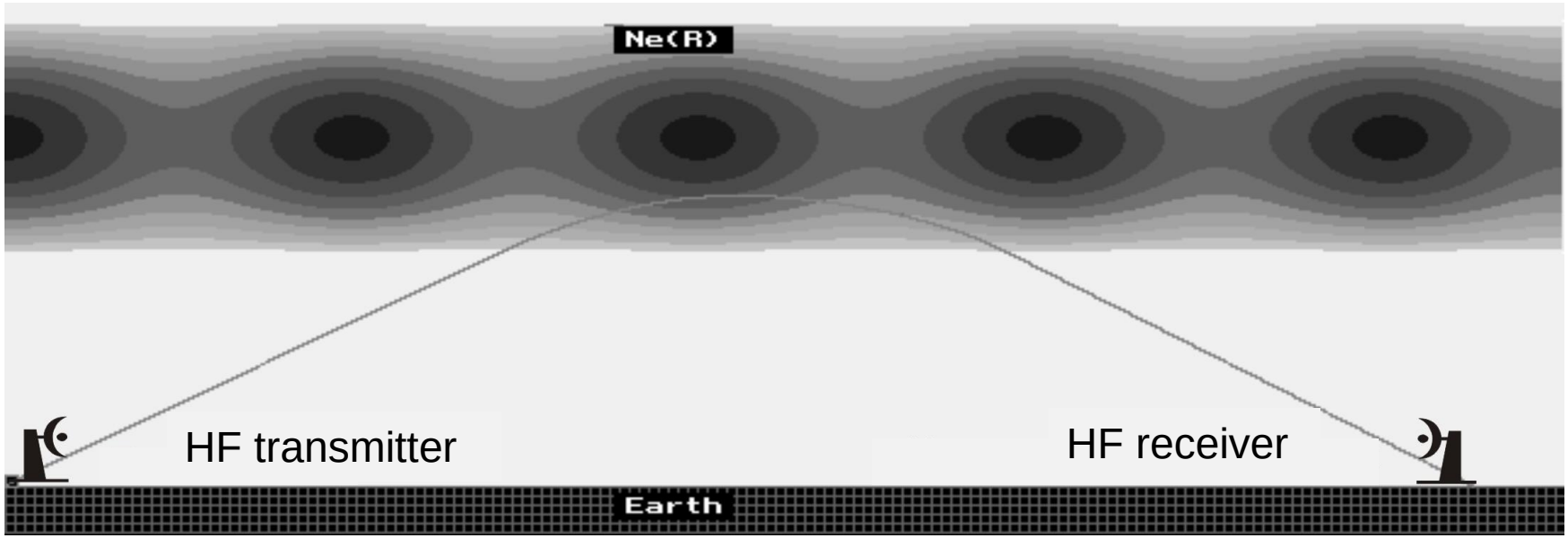

$$\Delta f = -\frac{f}{c}\frac{dP}{dt}, \quad P = \int_S n \cdot dS$$

Δf - Doppler frequency shift
P - Phase path of the wave in the ionosphere

Phase path ΔP varies because of changes of the:

1) Medium $n(t)$ - then: $\Delta f \sim \frac{1}{f}$

2) Variations of the ray trajectory $S(t)$ – then: $\Delta f \sim f$

n - refractive index
S - ray trajectory
f - signal frequency
c - velocity of light

Doppler frequency shift variations during solar eclipse, observed at Svalbard and in Kharkiv

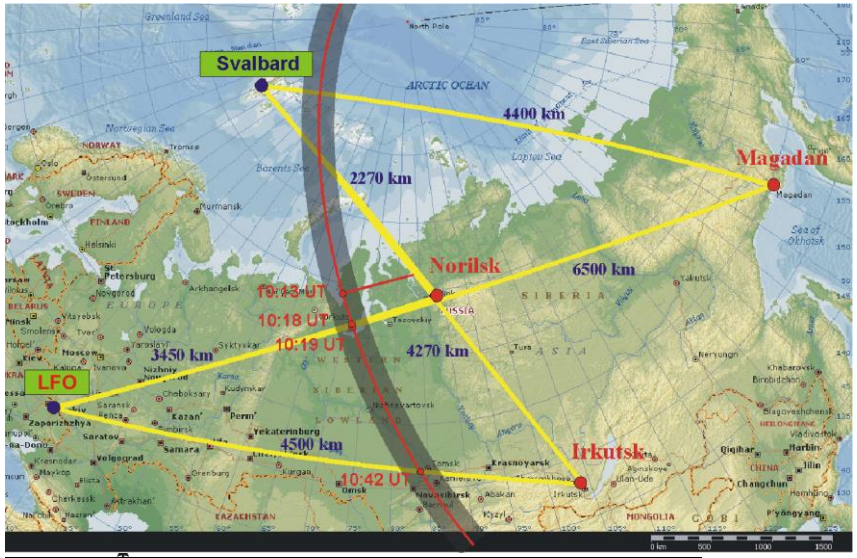

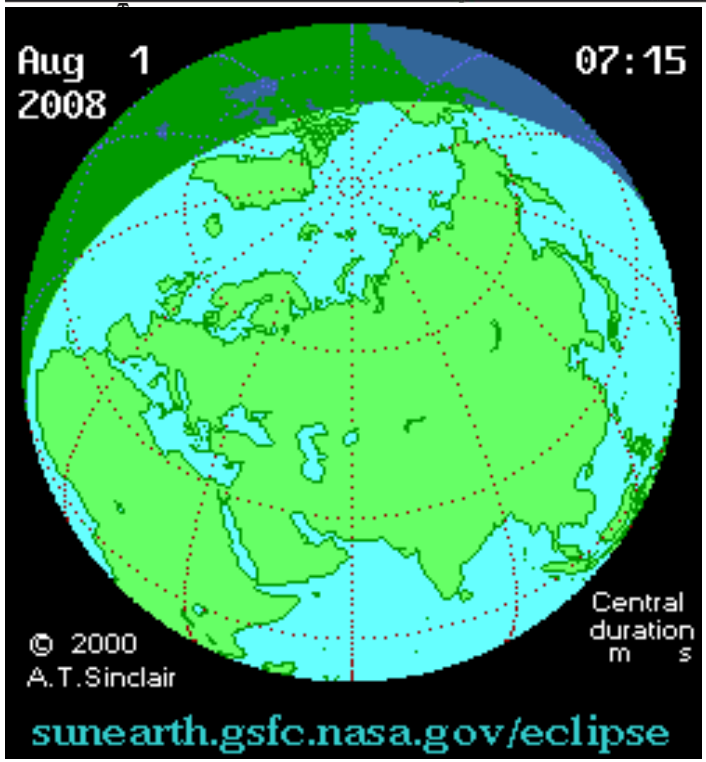

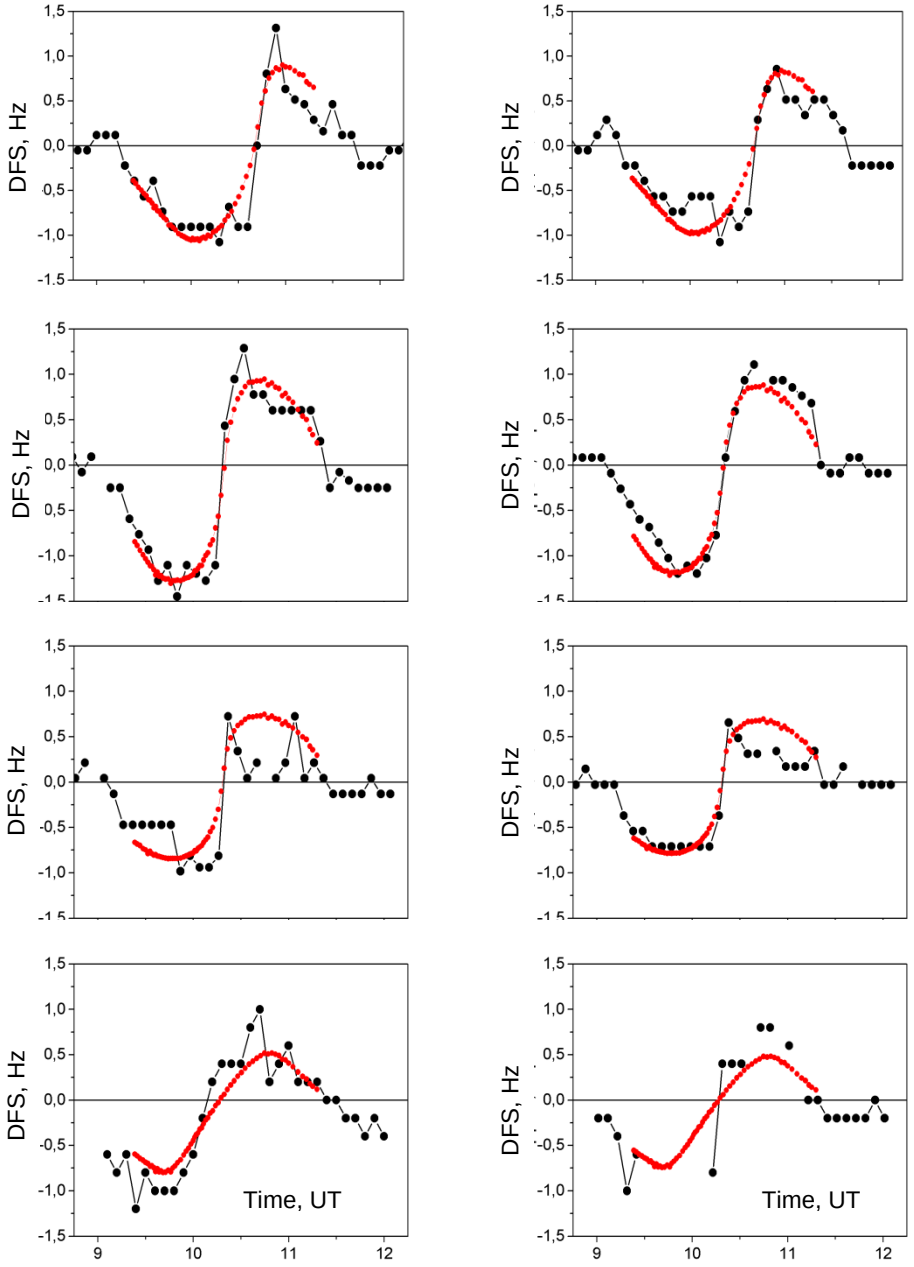

F = 10999 кГц

F = 12333 кГц

Self-scattering experiment

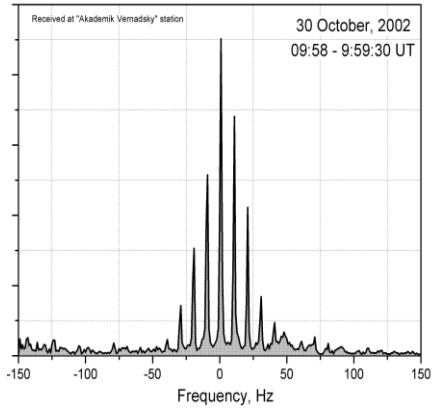

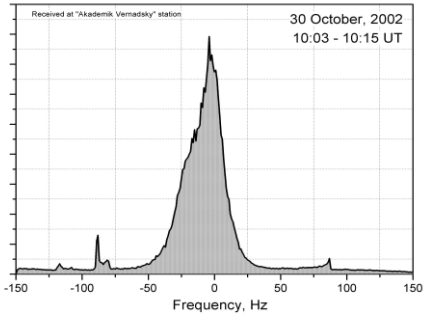

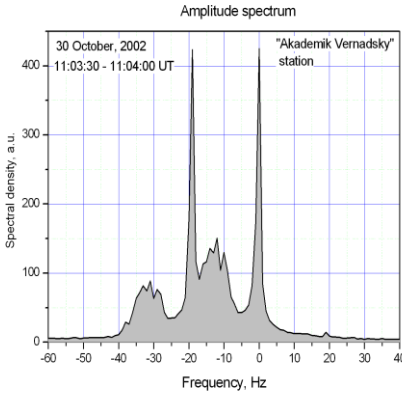

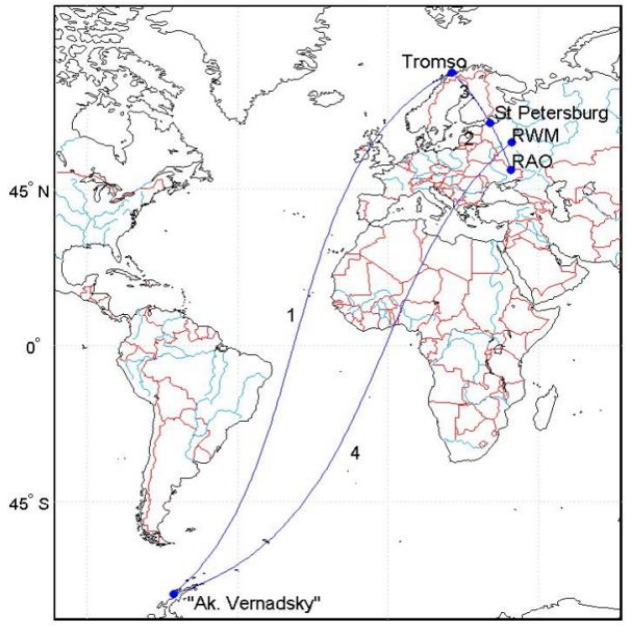

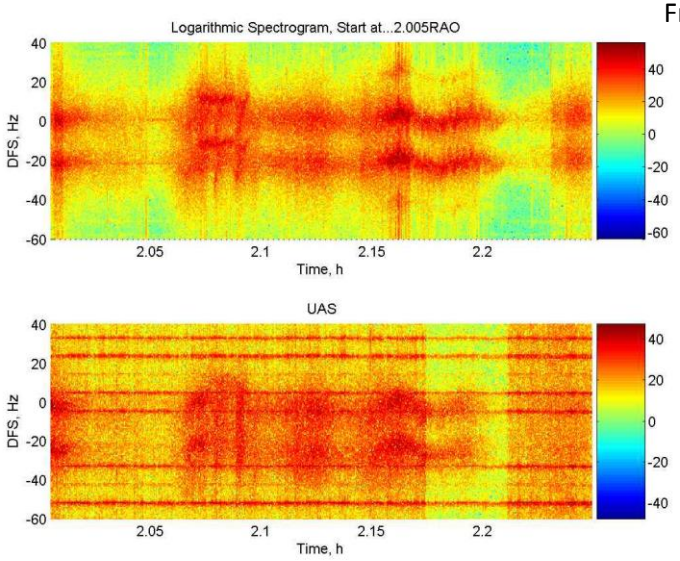

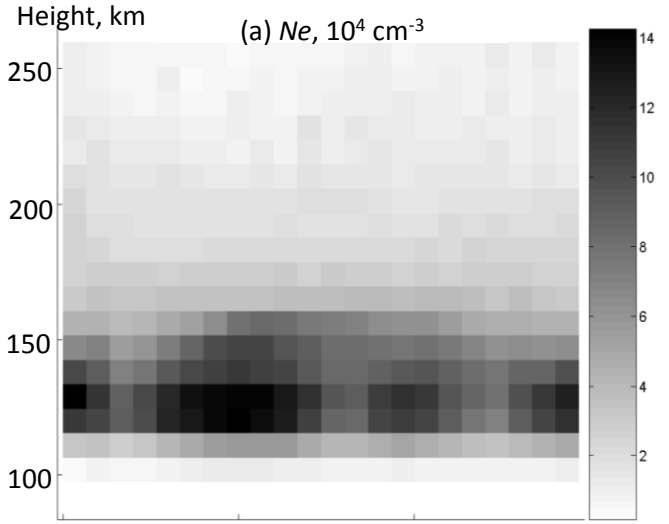

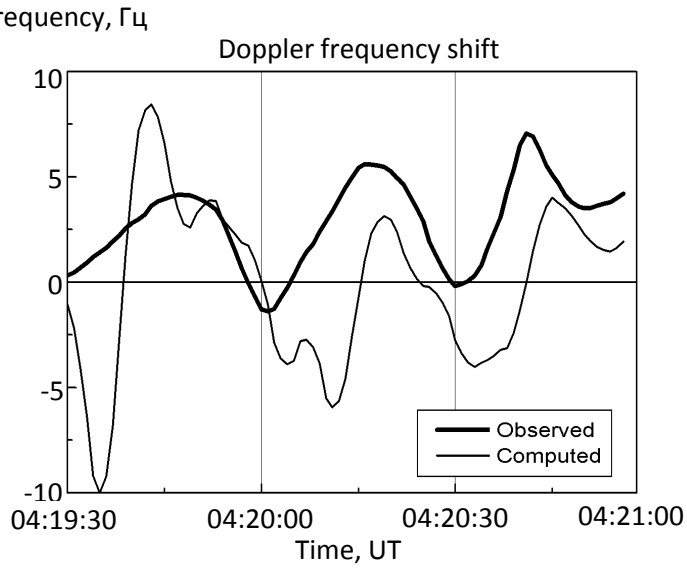

Monitoring of HF signals of RWM station situated near Moscow (Russia)

RWM -Tromso, 29-31.10.2014

4996 kHz

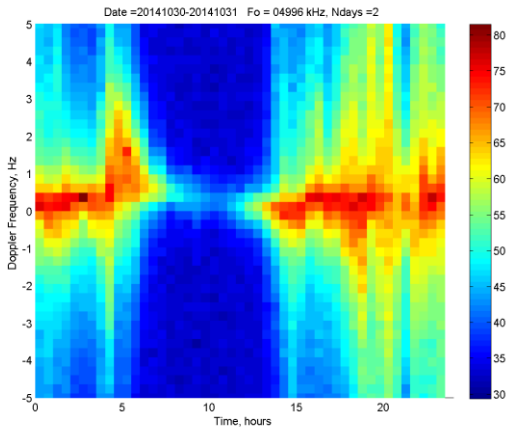

9996 kHz

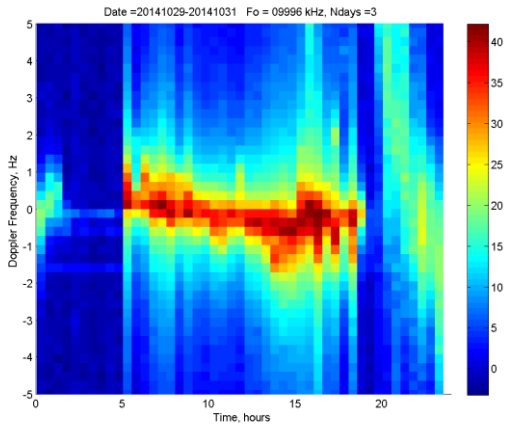

14996 kHz

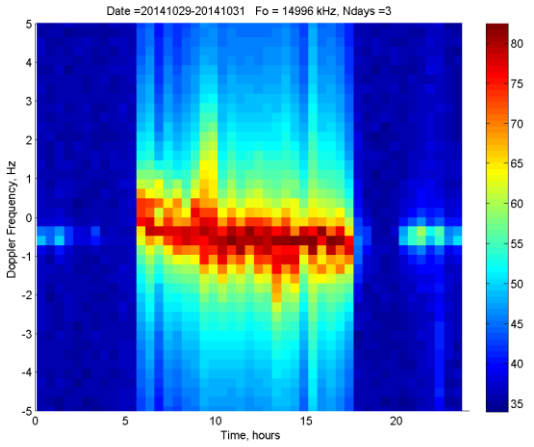

RWM-Svalbard, 29-31.10.2014

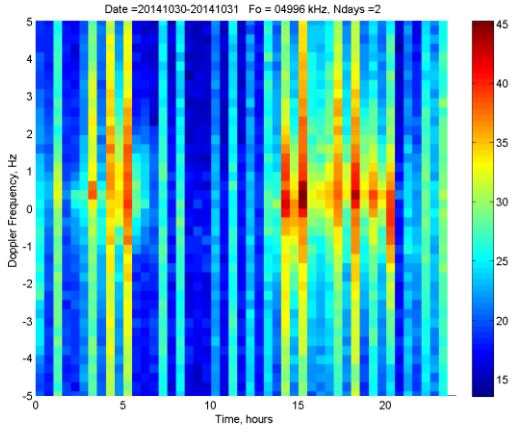

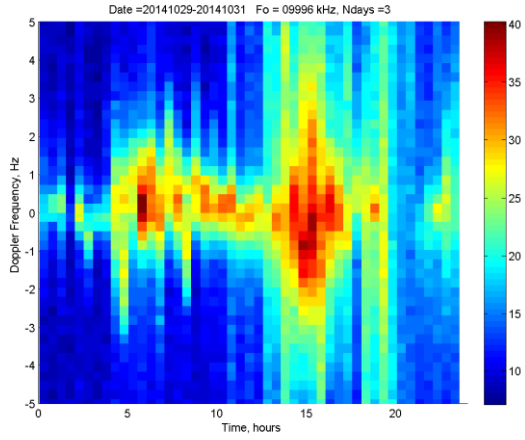

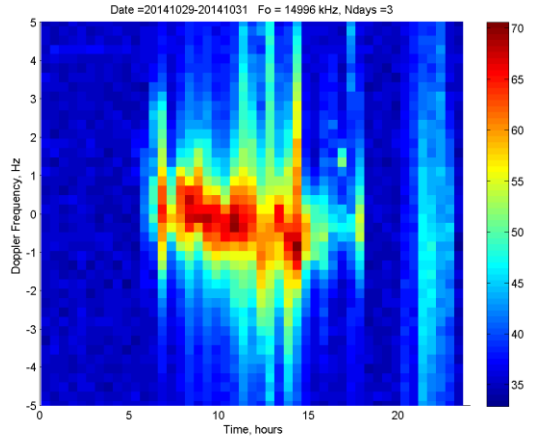

Doppler shift variations produced by gravity waves and geomagnetic pulsations

Spectrogram obtained during the transatlantic voyage to Ukrainian Antarctic station

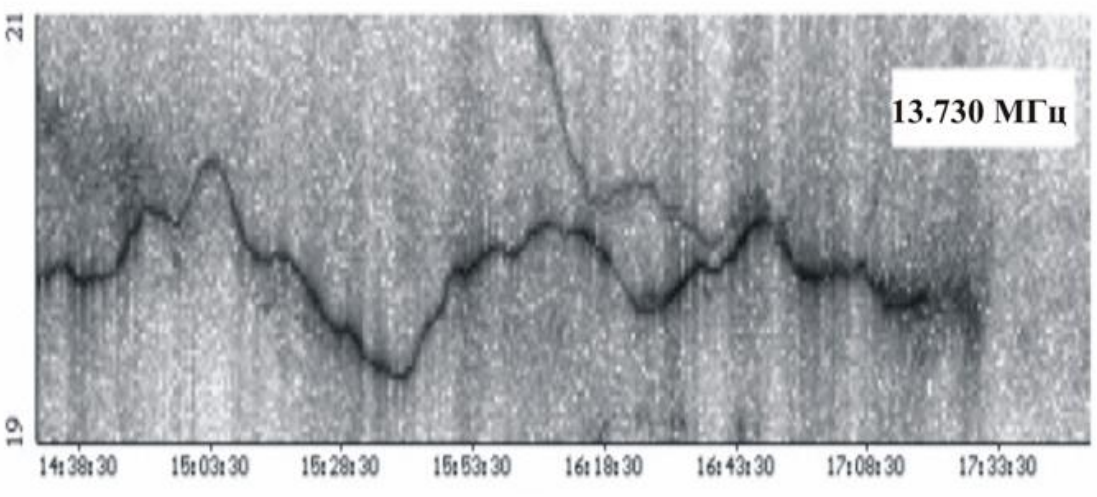

Radio path Abuja-Lagos (Nigeria), D~500 km

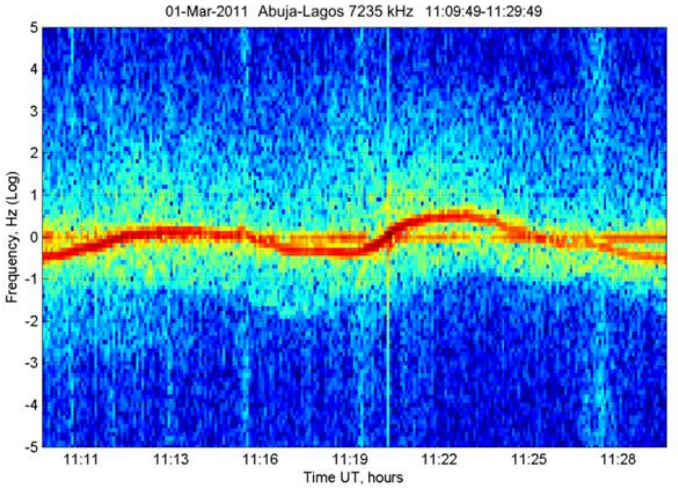

Radio path RWM-Tromso (Norway), D~ 1800 km

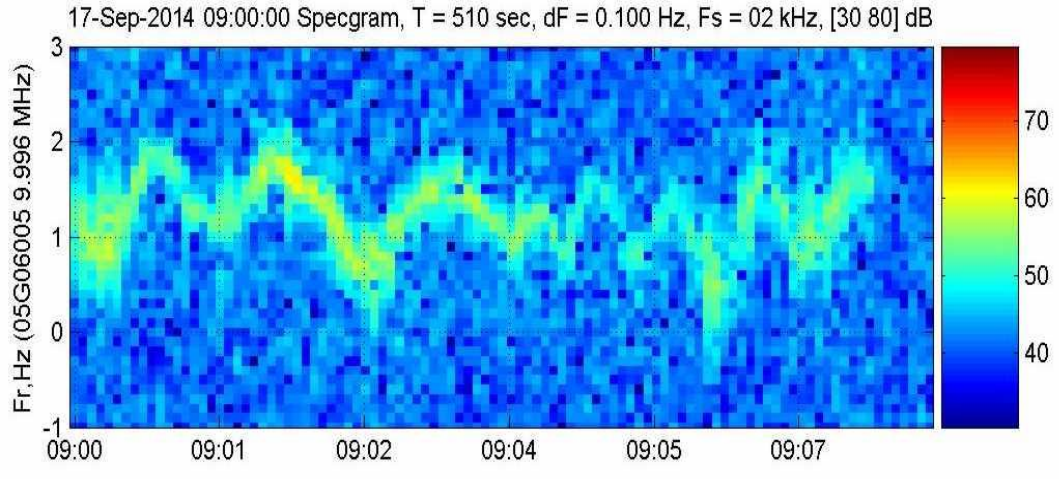

Radio path KHO-Hornsund (Svalbard), D~90 km

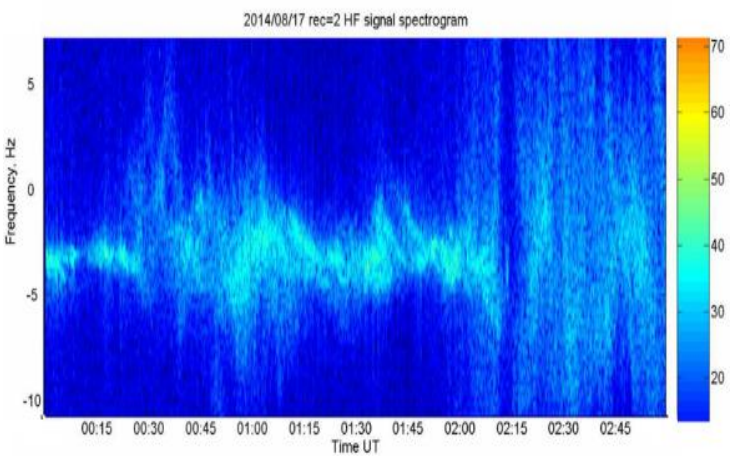

Traveling ionospheric disturbances (model)

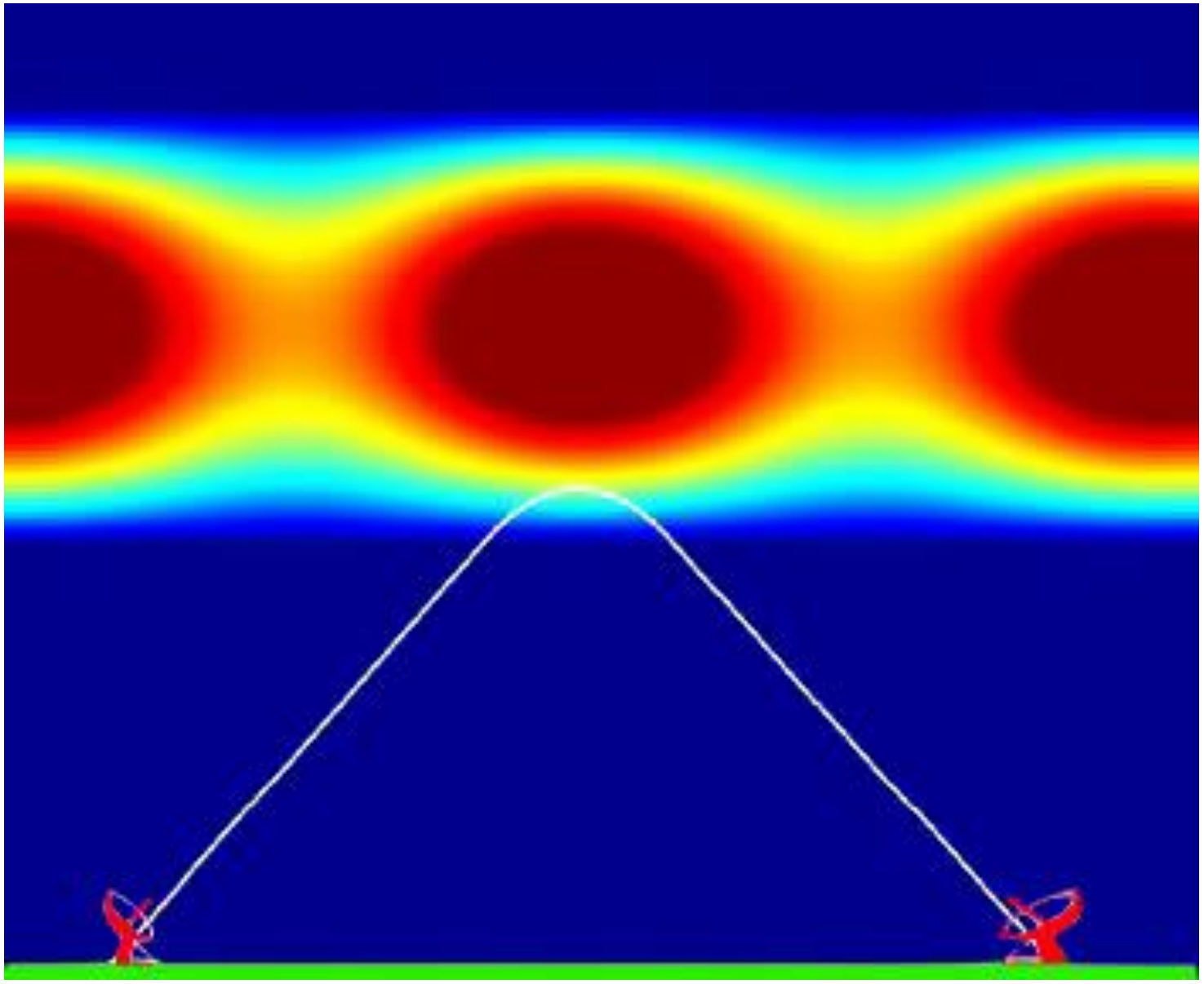

UTR-2 radio telescope

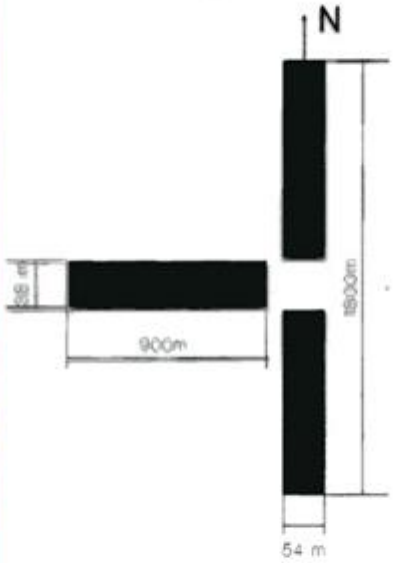

Location:
$49^0 39'$ N; $36^0 31'$ E

Range of frequencies:
10-32 MHz

Effective collected area
$S \approx 1.5 \times 10^5$ m^2 (at 25 MHz)

North-South (NS) antenna
1800 m × 54 m (1440 dipoles)
5 knife-like beams (NS1-NS5)

East West (EW) antenna
900 m × 38 m (600 dipoles)
1 knife-like beam (EW)

- All antennas are independently electrically steerable with a discrete step 0.2^0
- The characteristic pattern widths of the UTR-2 beams when phased toward heated volume $\Delta\varepsilon \sim 1^0$; $\Delta A \sim 1.5^0$

Frequency and Angular Sounding of the Ionosphere (FASI)

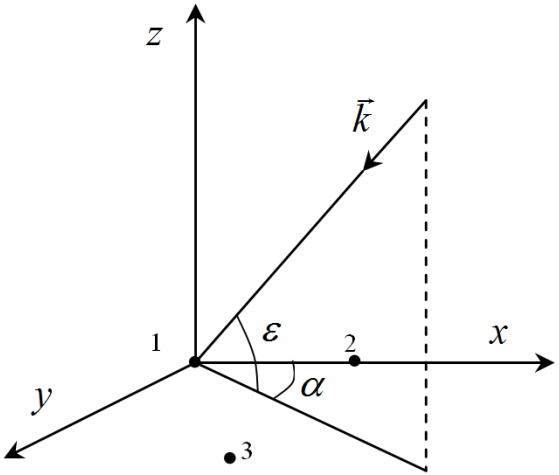

$$\tan\alpha = \frac{x_2\Delta\varphi_{3-1} - x_1\Delta\varphi_{2-1}}{y_3\Delta\varphi_{2-1}}$$

$$\cos\varepsilon = \frac{\Delta\varphi_{3-1}}{k(x_3\cos\alpha + y_3\sin\alpha)}$$

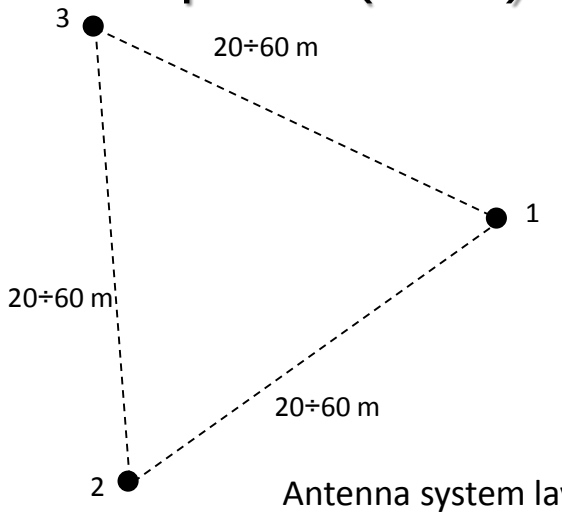

Antenna system layout

where $\Delta\varphi_{3-1}, \Delta\varphi_{2-1}$ are phase differences and k is wave vector.

Model of perfectly reflecting ionosperic surface

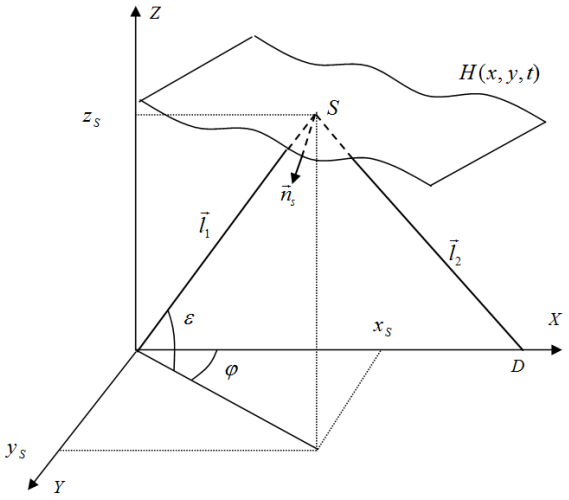

$$H(x,y,t) = H_o[1 + h(x,y,t)] \qquad |h| << 1$$

$$l_1 + l_2 = l \equiv c\cdot\tau_d \qquad \tan\alpha_x = \frac{\partial H}{\partial x} \equiv \gamma_x \qquad \tan\alpha_y = \frac{\partial H}{\partial y} \equiv \gamma_y$$

$$|\gamma_x|, |\gamma_y| << 1$$

$$\frac{l\cdot\cos\varepsilon\cdot\cos\varphi - D}{\sqrt{D^2 + l^2 - 2\cdot D\cdot l\cdot\cos\varepsilon\cdot\cos\varphi}} = -\gamma_x \qquad \frac{l\cdot\cos\varepsilon\cdot\sin\varphi}{\sqrt{D^2 + l^2 - 2\cdot D\cdot l\cdot\cos\varepsilon\cdot\cos\varphi}} = -\gamma_y$$

$$F_D = -\frac{1}{\lambda}\frac{dl}{dt} \qquad X_s = -\gamma_x \qquad Y_s = -\gamma_s \qquad F_D = -\frac{4H_0^2}{\lambda\cdot l_0}\cdot\frac{dh}{dt}$$

Frequency and Angular Sounding of the Ionosphere (FASI)

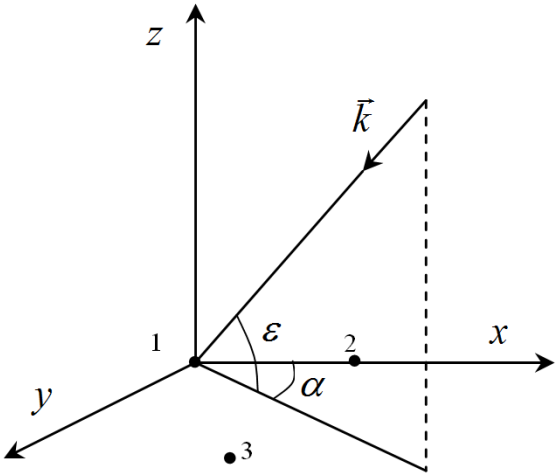

$$\tan\alpha = \frac{x_2\Delta\varphi_{3-1} - x_1\Delta\varphi_{2-1}}{y_3\Delta\varphi_{2-1}}$$

$$\cos\varepsilon = \frac{\Delta\varphi_{3-1}}{k(x_3\cos\alpha + y_3\sin\alpha)}$$

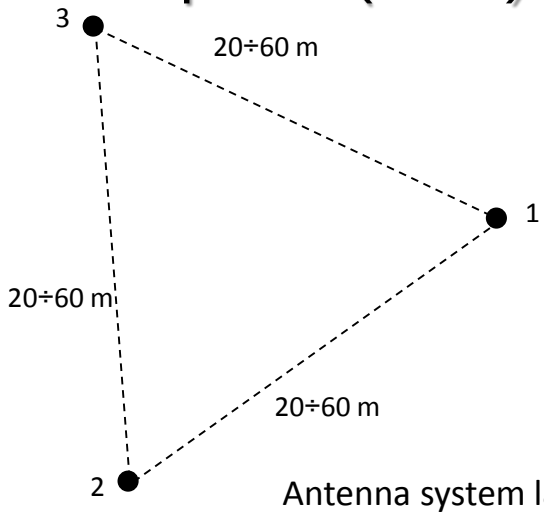

Antenna system layout

where $\Delta\varphi_{3-1}, \Delta\varphi_{2-1}$ are phase differences and k is wave vector.

Model of density waves propagating in a ionospheric layer

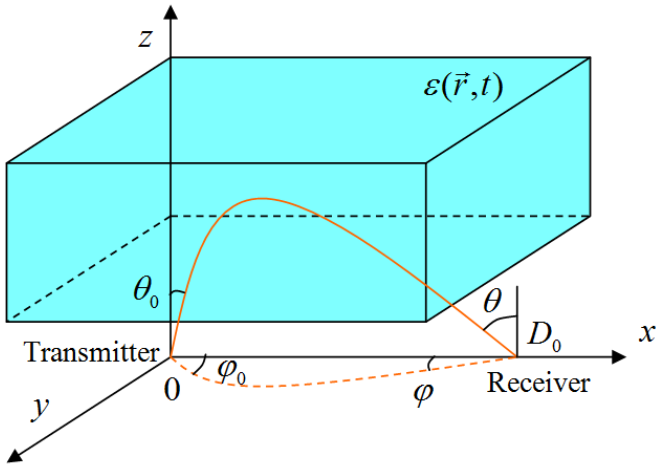

$$\varepsilon(\vec{r},t) = \varepsilon_0(z) + \varepsilon_1(\vec{r},t) \qquad |\max\varepsilon_1| << \varepsilon_0$$

$$\varepsilon_0(z) = 1 - \alpha^2 \cdot F(z) \qquad \Phi(z)$$

height profile of the disturbances amplitude

$$\varepsilon_1(\vec{r},t) = \Phi(z)\cdot\nu(\vec{r},t) \qquad \nu(\vec{r},t)$$

3D disturbance waveform

$$\alpha = f_{cr}/f_0 \qquad L = L_0 + L_1 \qquad L_0 = \int_0^{D_0/\sin\theta_0} \varepsilon_0(z(\rho))d\rho \qquad L_1 = \frac{1}{2}\int_0^{D_0/\sin\theta_0} \varepsilon_1(\vec{r}(\rho),t)d\rho$$

$$F_D = -\frac{1}{\lambda}\frac{\partial L_1}{\partial t} \qquad \Delta\varphi \approx -\frac{1}{D_0\sin\theta_0}\frac{\partial L_1}{\partial\varphi_0} \qquad \Delta\theta \approx \frac{1}{\cos\theta_0(\partial D/\partial\theta_0)}\frac{\partial L_1}{\partial\theta_0}$$

Low-cost FASI complex based on Winradio G3131i and antenna switch

Ovenized crystal oscillator

Antenna switch

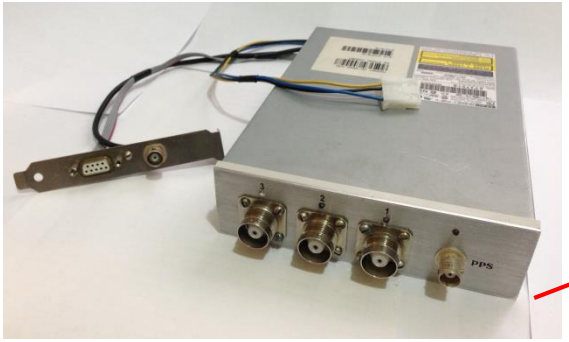

HF receiver

PC

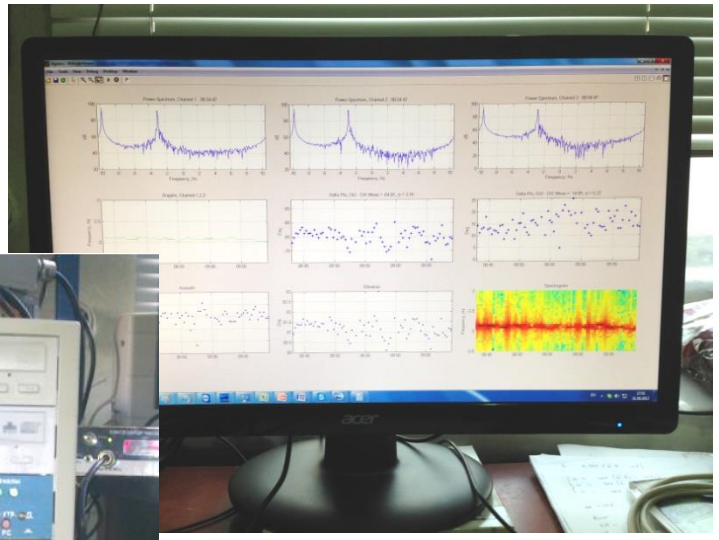

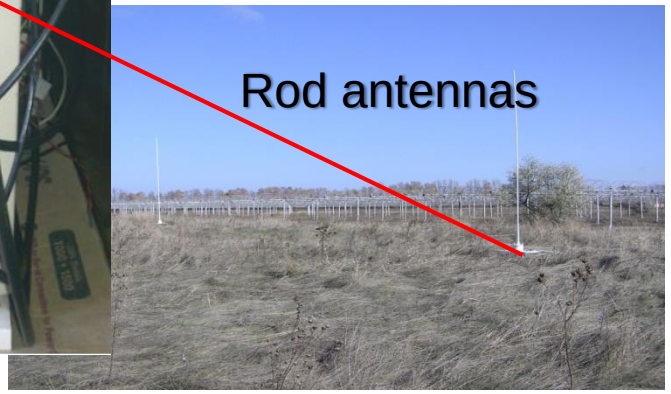

Rod antennas

Minsk – Kharkiv, D~700 km

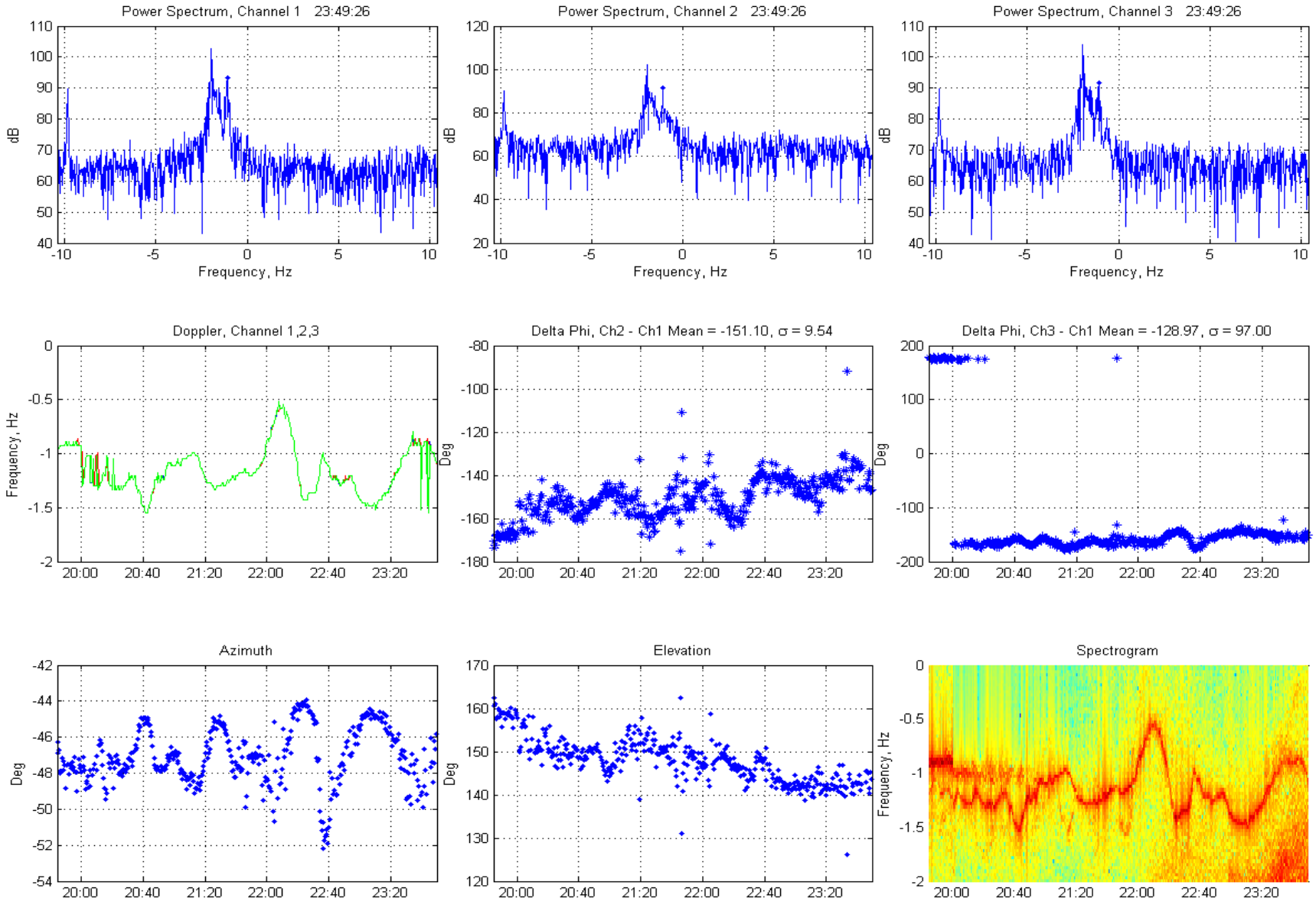

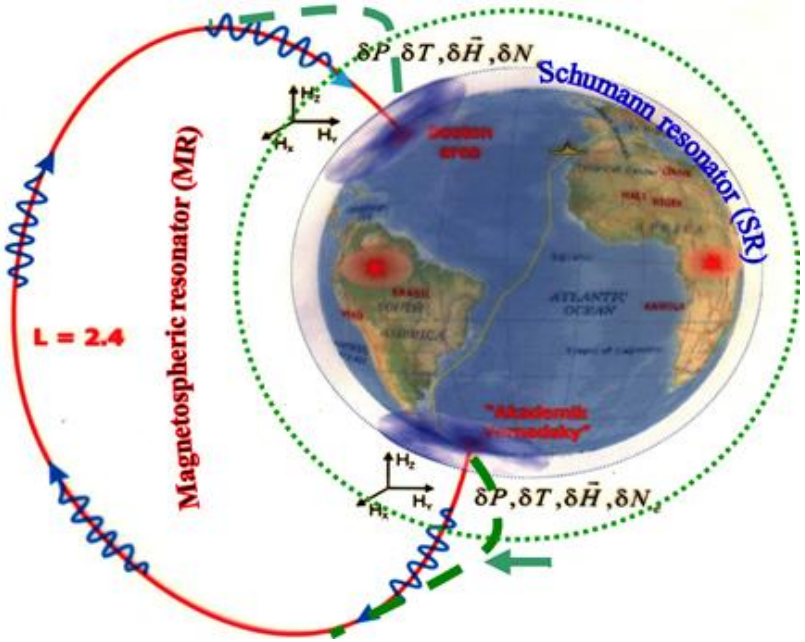

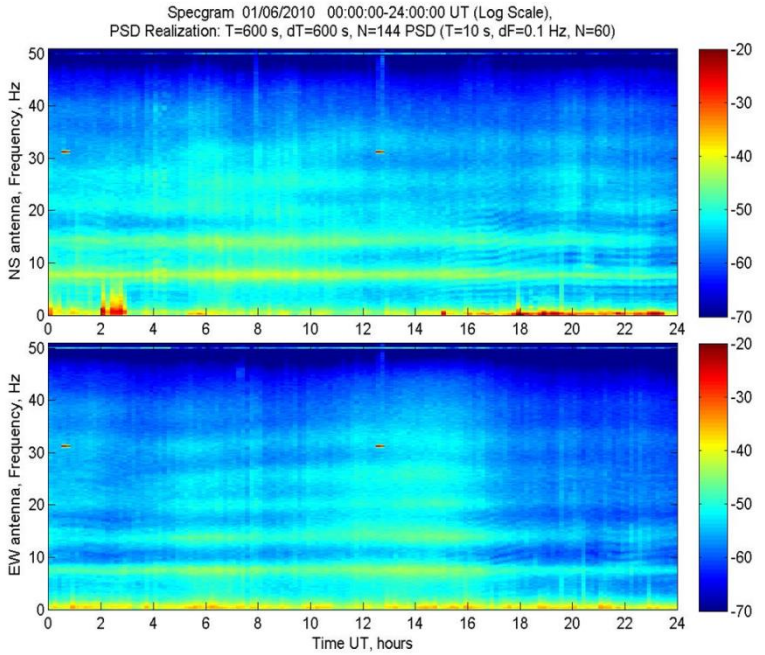

Typical spectrum of ELF signal measured at Vernadsky

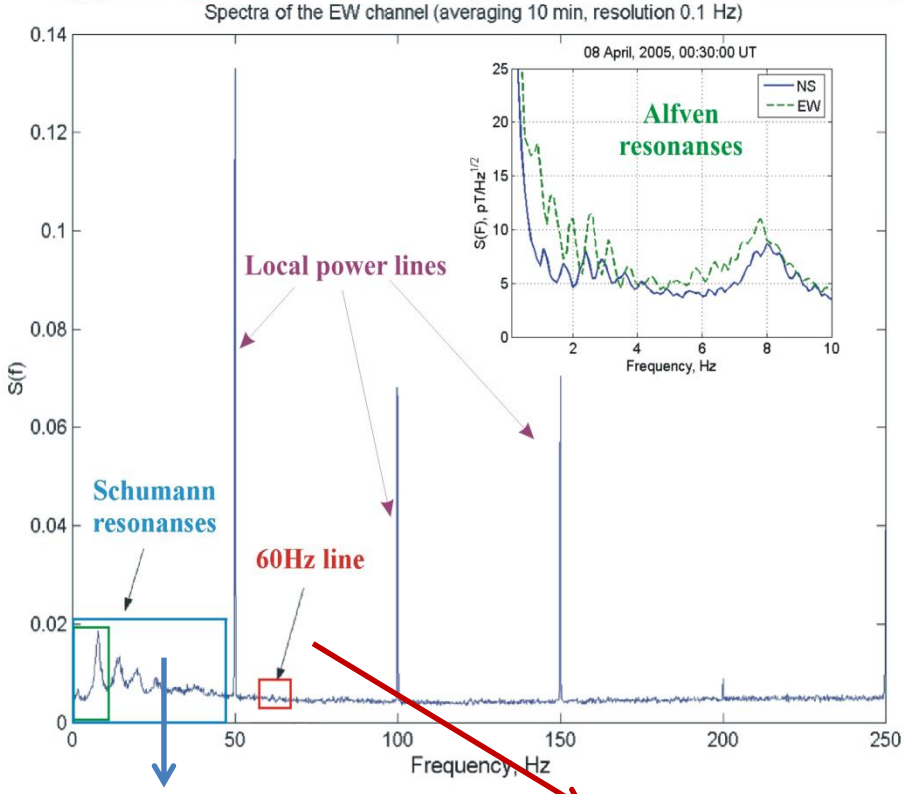

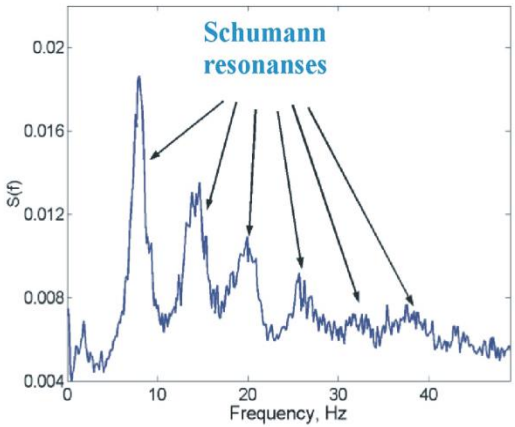

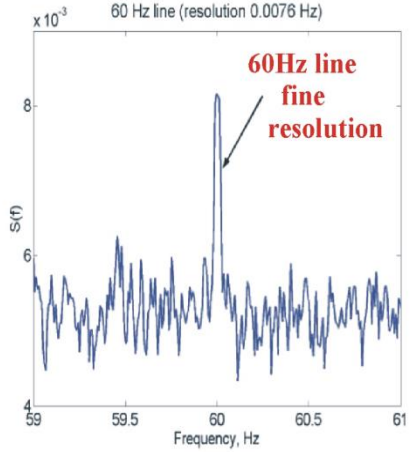

SR

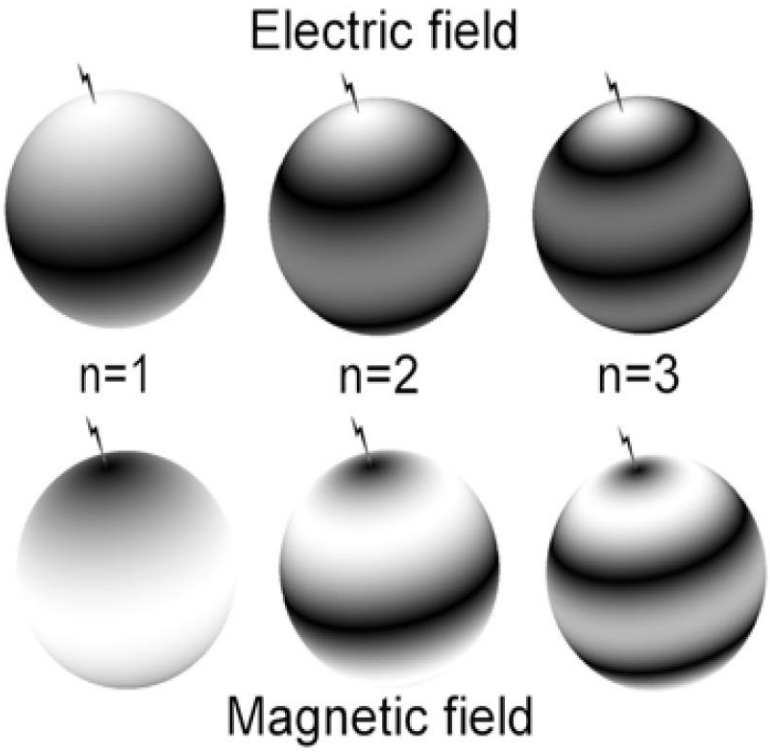

Electric and magnetic fields of the first three SR modes.

IAR

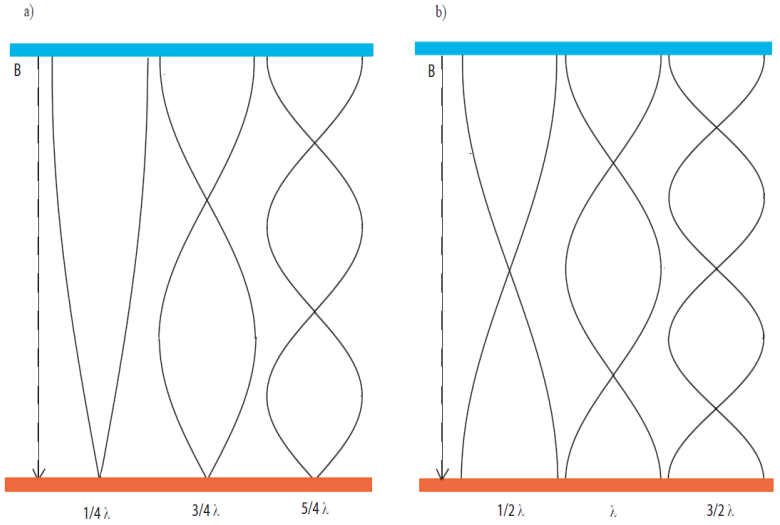

Fig Diagram showing an Alfvén wave's perpendicular electric field for the first 3 eigenmodes trapped in the IAR for the high conductivity ionosphere (panel **(a)**) and low conductivity (panel **(b)**) ionosphere. The lower red rectangles represent the lower IAR boundary and the blue rectangle represents the upper IAR boundary.

Locations of the ELF waveband magnetometers and animation demonstrating distribution of lightning flashes (OTD satellite data)

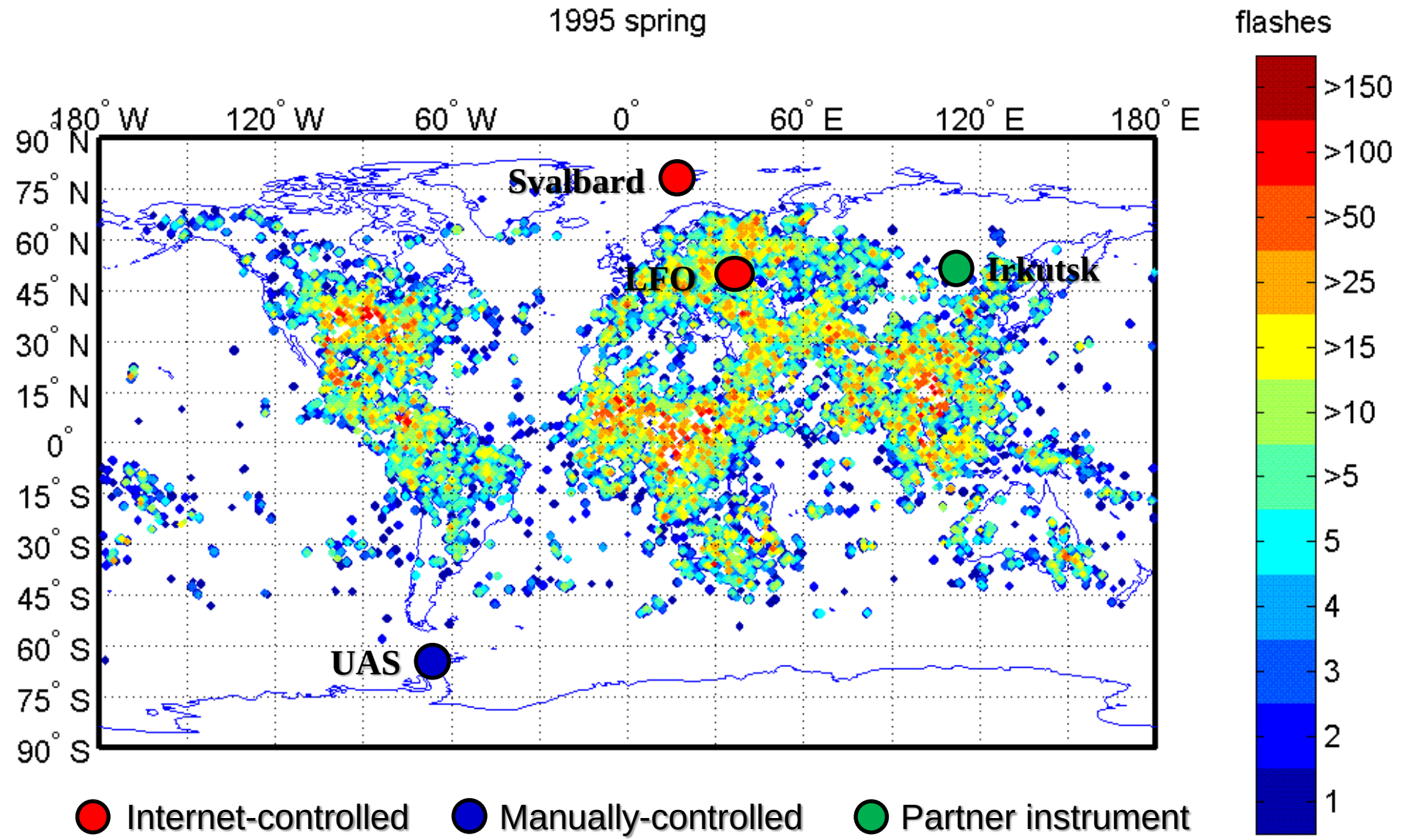

Lightning is a main source of SR and IAR

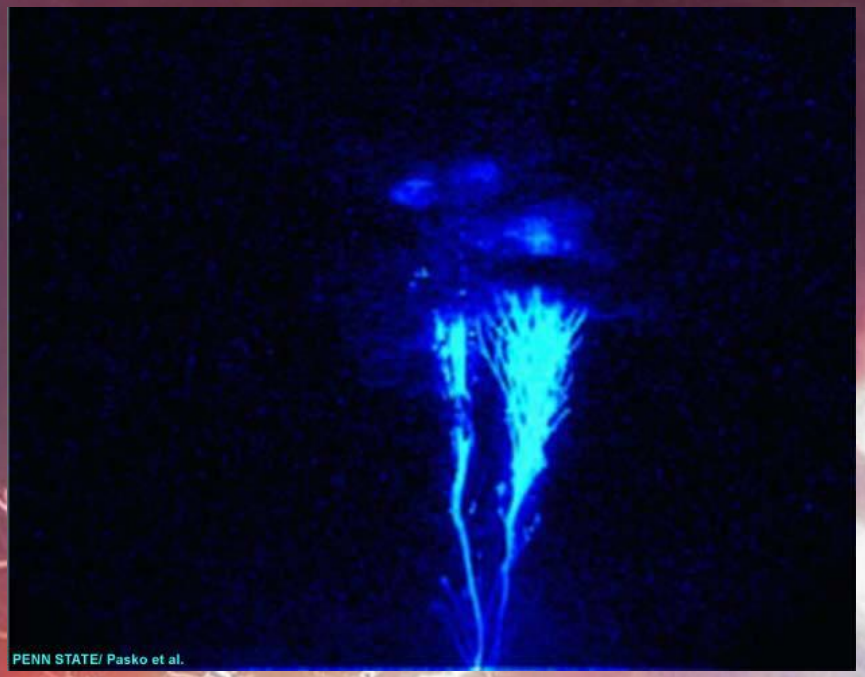

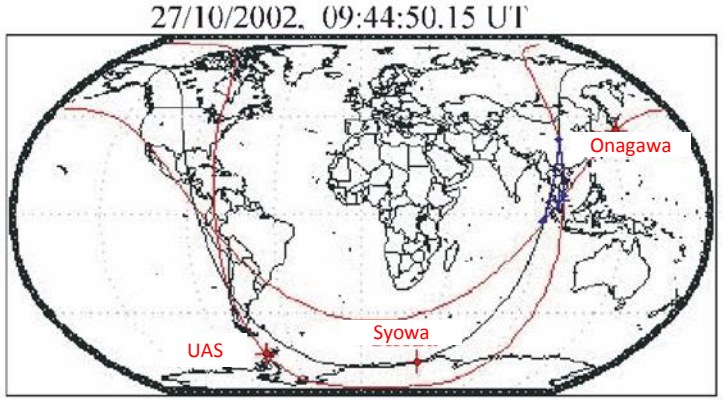

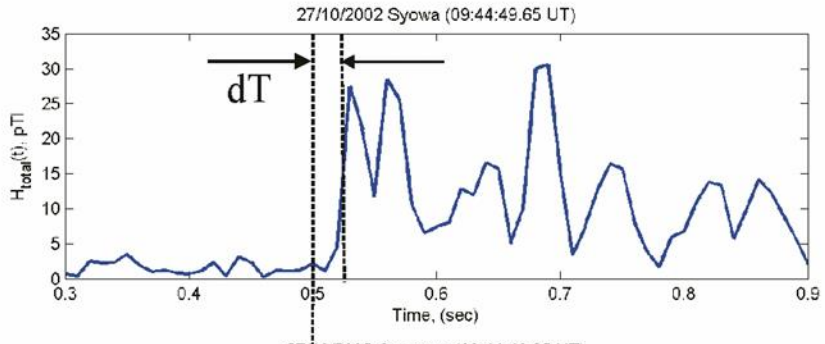

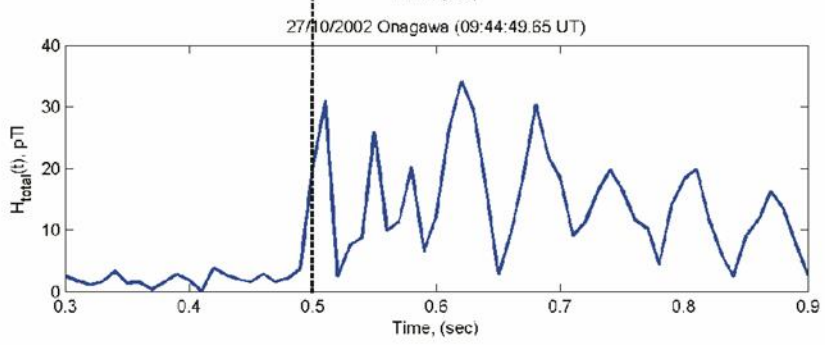

October 27-30, 2002

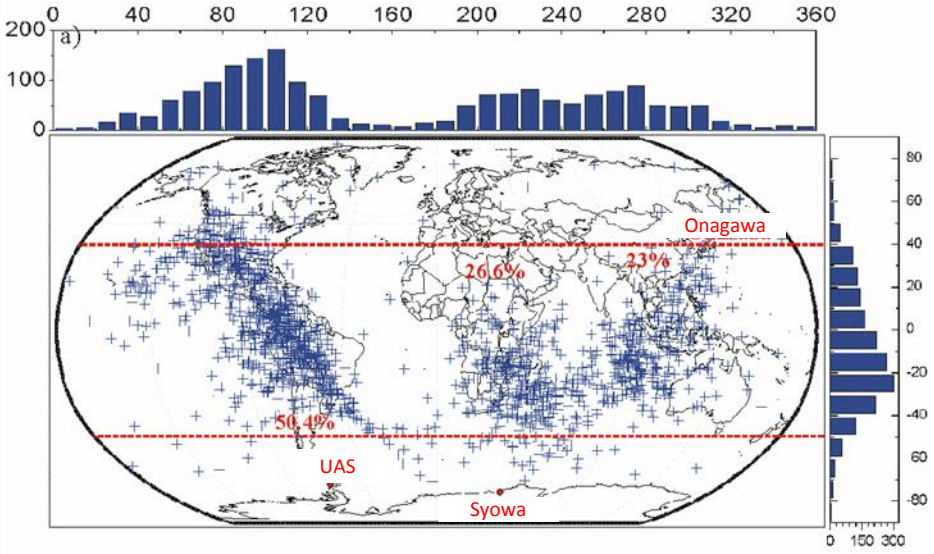

(Lightning Imaging Sensor), http://thunder.msfc.nasa.gov/data/lisbrowse.html.

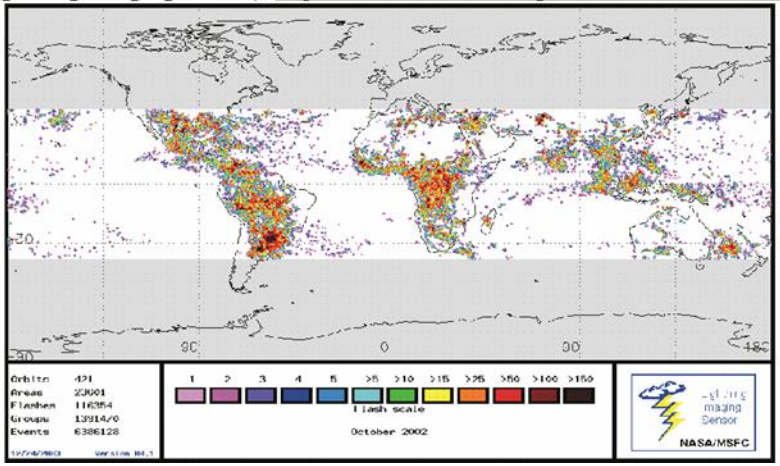

Spectral and polarization technique of data processing

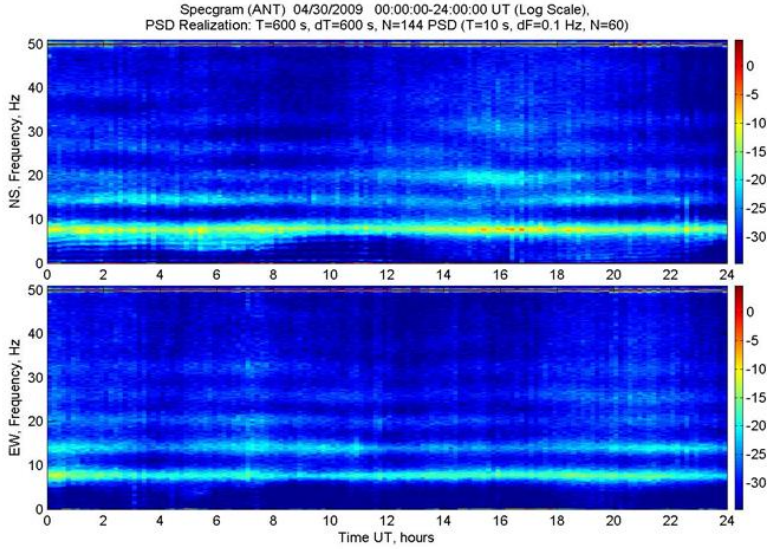

Diurnal record is divided on intervals dT. For each interval power spectra S_{xx}, S_{yy} and cross-spectrum S_{xy} are calculated

$$S_{ik}(f) = \frac{1}{N}\sum_{p=1}^{N} \tilde{H}_i^{(p)}(f)\tilde{H}_k^{(p)*}(f)$$

Instantaneous spectra $\tilde{H}_{i,k}^{(p)}(f)$ corresponding to the intervals $(p-1)T \le t \le pT$; $p = 1,2,..N$, $N \cdot T = dT$ are determined by

$$\tilde{H}_{i,k}^{(p)}(f) = \frac{1}{T}\int_{(p-1)T}^{pT} dt H_{i,k}(t) e^{-i2\pi ft}$$

Stockes parameters are calculated

$$I(f) \equiv S_{xx}(f) + S_{yy}(f), \qquad Q(f) \equiv S_{xx}(f) - S_{yy}(f),$$

$$U(f) \equiv 2\,\mathrm{Re}\,S_{xy}(f), \qquad V(f) \equiv 2\,\mathrm{Im}\,S_{xy}(f)$$

and used for determination of the:

$r(f)$ - Ellipticity

$\Psi(f)$ - Polarization angle

$I_p(f)$ - Polarized intensity

$P(f)$ - Degree of polarization

$$r = \frac{V}{\sqrt{Q^2+U^2} + \sqrt{Q^2+U^2+V^2}},$$

$$\left.\begin{matrix}\sin(2\Psi)\\ \cos(2\Psi)\end{matrix}\right\} = \frac{1}{\sqrt{Q^2+U^2}}\begin{cases}U\\ Q\end{cases},$$

$$I_p = \sqrt{Q^2+U^2+V^2},$$

$$P = I_p / I.$$

Intensities and position angle of SR signals

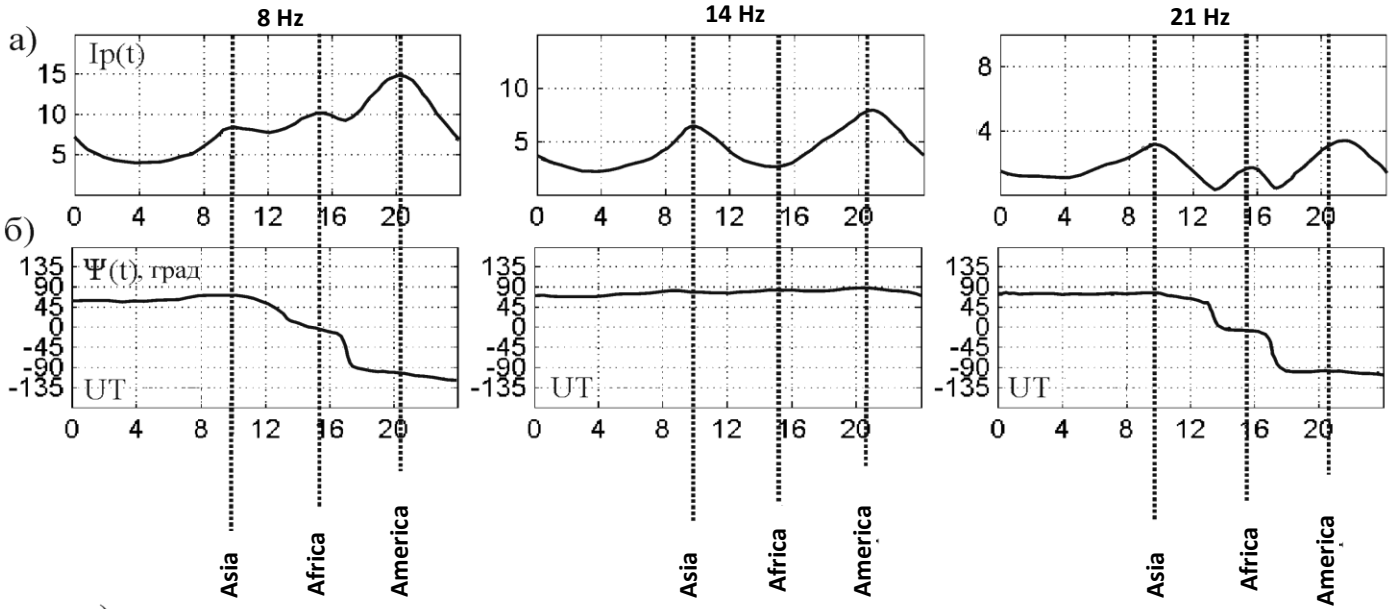

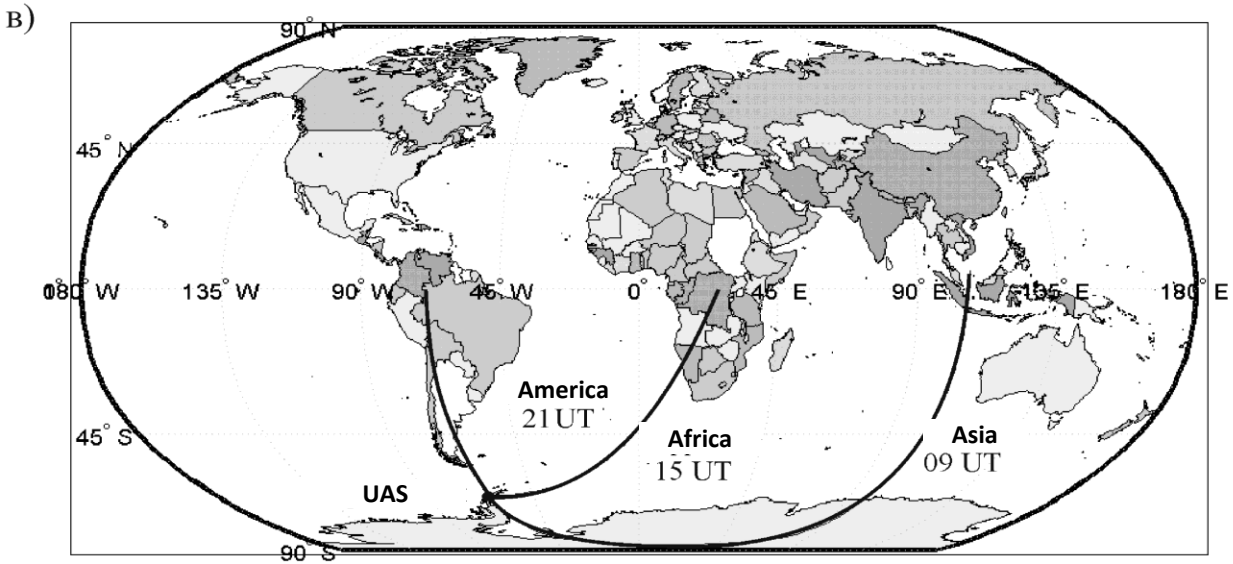

Calculation of the activities of the world lightning centers

In the frame of asymptotic theory of fields of the Schumann resonance in the gyrotropic Earth-ionosphere cavity

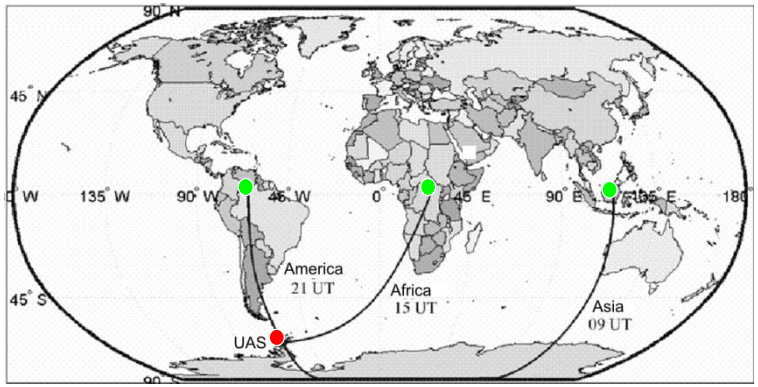

- Lightning activity is concentrated in 3 points centers at the equator
- The Earth surface is perfectly conducted
- Gyrotropic ionosphere with high-conductivity boundary is described by the tensor the of the surface impedance Z with small diagonal element $|Z_{ik}|<<1$
- Activities of Asia – A_1 and Africa+America – A_2+A_3 lightning centers are calculated

Impedance of the isotropic ionosphere Z_0 and the ratio of the off-diagonal and diagonal elements of the matrix of the surface impedance of the gyrotropic ionosphere Z_2/Z_1 are used as small parameters

$$A_1^{(1)}(t)=\frac{1}{2}\left[A_+^{(1)}(t)+A_-^{(1)}(t)\right]$$ - Africa

$$\left[A_2^{(1)}(t)+A_3^{(1)}(t)\right]=\frac{1}{2}\left[A_+^{(1)}(t)-A_-^{(1)}(t)\right]$$ - Asia + America

$$\rho\equiv\frac{\omega_H}{\nu_e}=\frac{1.5\cdot\Delta\lambda^{(1)}}{(0.75)^2-\left(\Delta\lambda^{(1)}\right)^2}$$ - Parameter of gyrotropy

где: $$A_+^{(1)}(t)=\frac{1}{2\sin^2\Phi}\left\{I_p\left(f^{(1)},t\right)\left(1+\sin^2\Phi\right)-Q\left(f^{(1)},t\right)\cos^2\Phi\right\}$$

$$A_-^{(1)}(t)=\left\{I_p\left(f^{(1)},t\right)\cos^2\Phi-Q\left(f^{(1)},t\right)\left(1+\sin^2\Phi\right)\right\}\begin{cases}1/2\sin^2\Phi\sin 2\left(\lambda-\hat{\lambda}_1^{(1)}\right)-\text{gyrotropic cavity}\\ 1/2\sin^2\Phi\sin 2\left(\lambda-\lambda_1\right)-\text{isotropic cavity}\end{cases}$$

$$\Delta\lambda^{(1)}=-\frac{V\left(f^{(1)},t\right)}{2A_+^{(1)}\sin\Phi}$$ - «apparent» angle shift of Africa source to the west $\hat{\lambda}_1^{(1)}=\lambda_1-\Delta\lambda^{(1)}$

$A_j^{(1)}(t)$ - electromagnetic activity (j-source) for first Schumann frequency

$\{\Phi;\lambda\}$ - observation point coordinates $\{\Phi_j=0;\lambda_j\}$ - lightning center coordinates.

$$A_j(t)\equiv\left[\frac{3c}{4\pi^2a^3f^{(1)}|z_1|}\right]^2<\left|\tilde{M}_j(t)\right|^2>$$ - electromagnetic activity (j-source), where a - Earth radius, c - speed of light,

$f^{(1)}$ - frequency of first maximum in the point of source

$<\left|\tilde{M}_j(t)\right|^2>$ - mean square of the current moment of j-discharge

$$z_1=\frac{z_0}{\sqrt{2}}\sqrt{1+\sqrt{1+\rho^2}}$$ - diagonal element of the impedance

$$z_0=\sqrt{\frac{i\omega\nu_{eff}}{\omega_0^2}}$$ - impedance of the isotropic ionosphere

ω_0 - critical frequency of the ionosphere

ω_H - ion gyro frequency

ν_{eff} - electron collision frequency

Diurnal and seasonal variation of the activities of world lightning centers

(A_1+A_{23} – Total activity , A_1 – Africa, A_{23} – Asia + America)

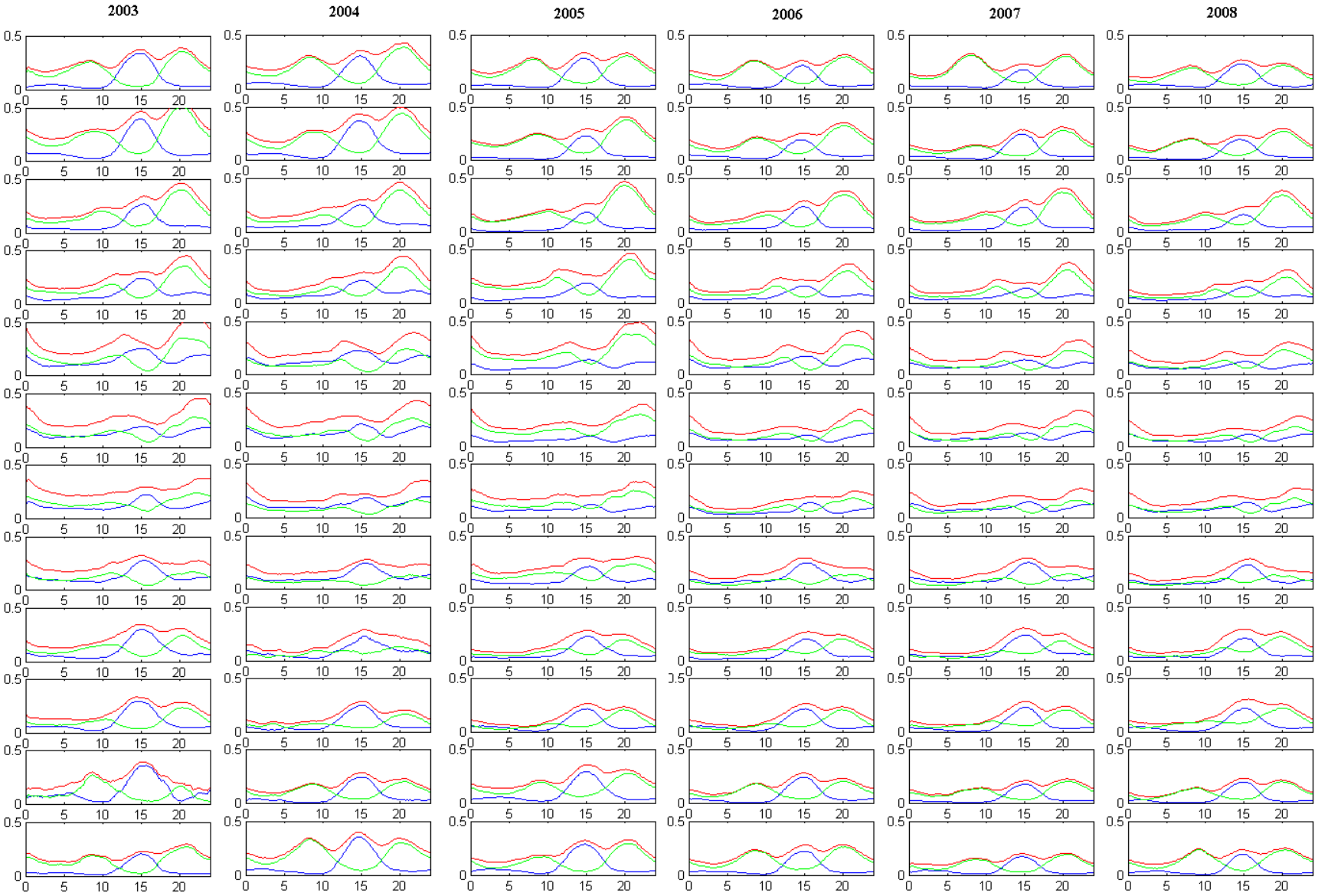

Parameters calculated within 11-years solar cycle

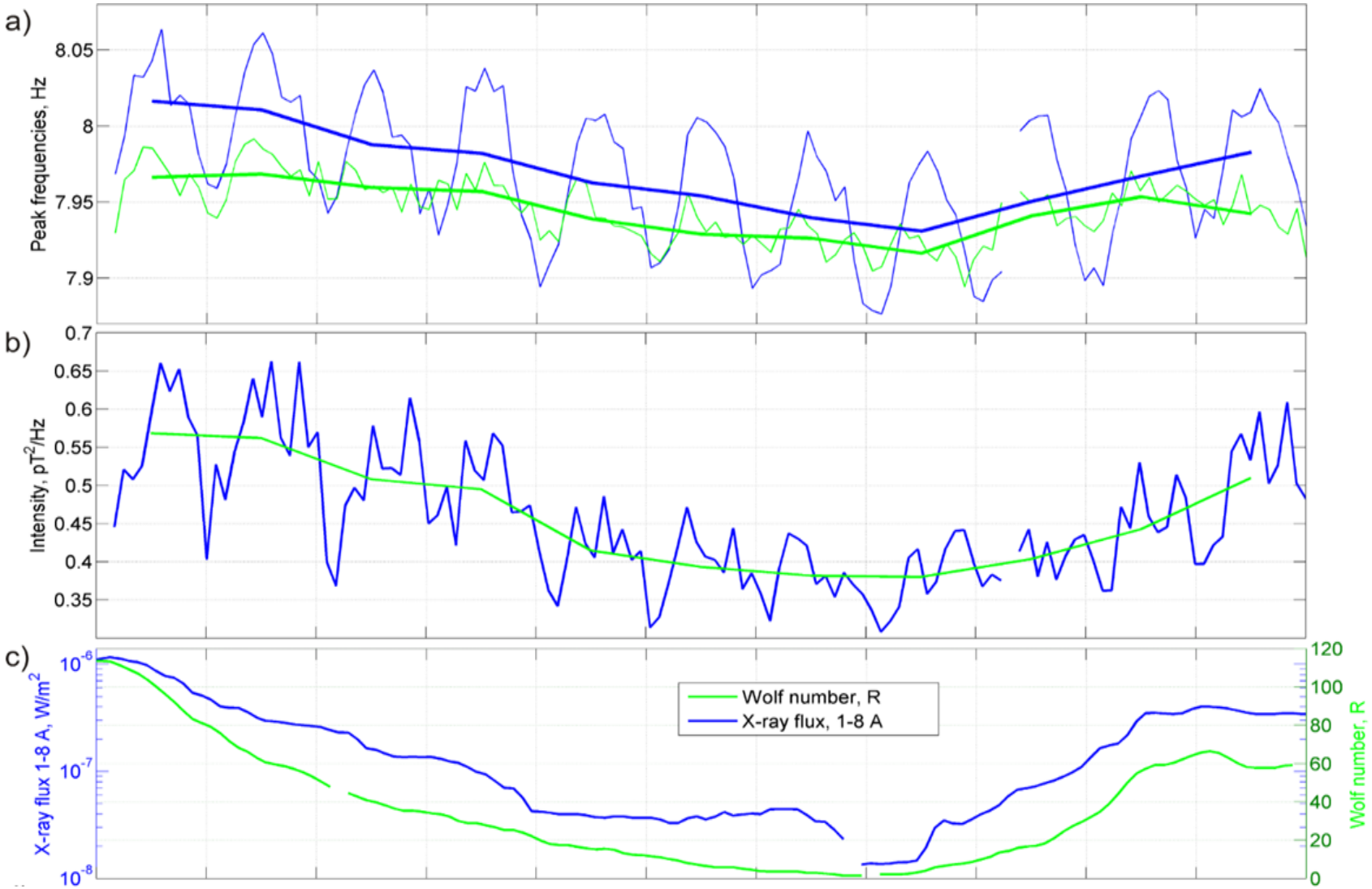

Estimation of the characteristics of Schumann resonance signal sources

Distributions of the numbers of flashes

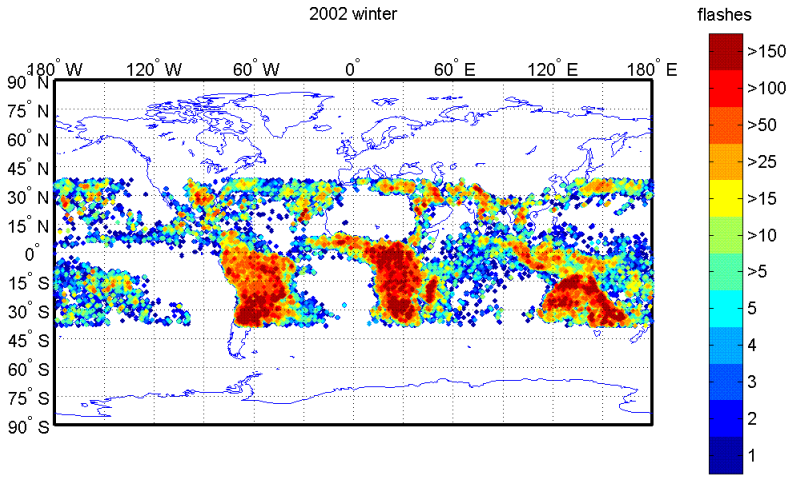

Variation of the number of flashes calculated with satellite data (Lightning Imaging Sensor (LIS) data: https://amser.org/index.php?P=AMSER--ResourceFrame&resourceId=4353

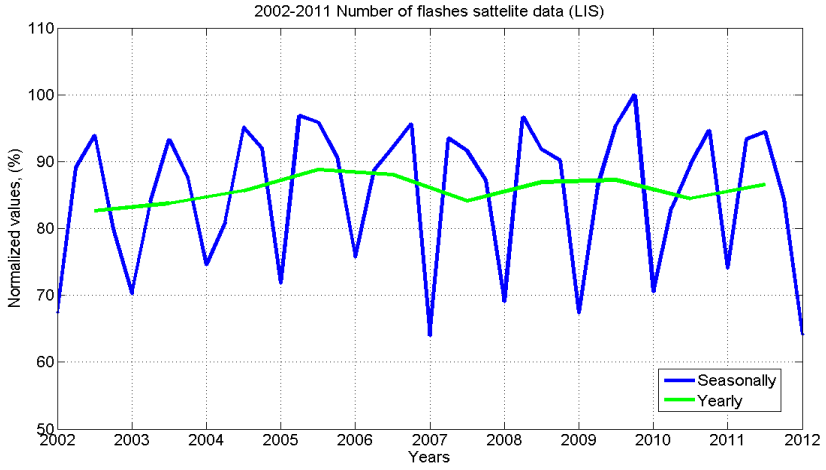

Map of the meteorological stations

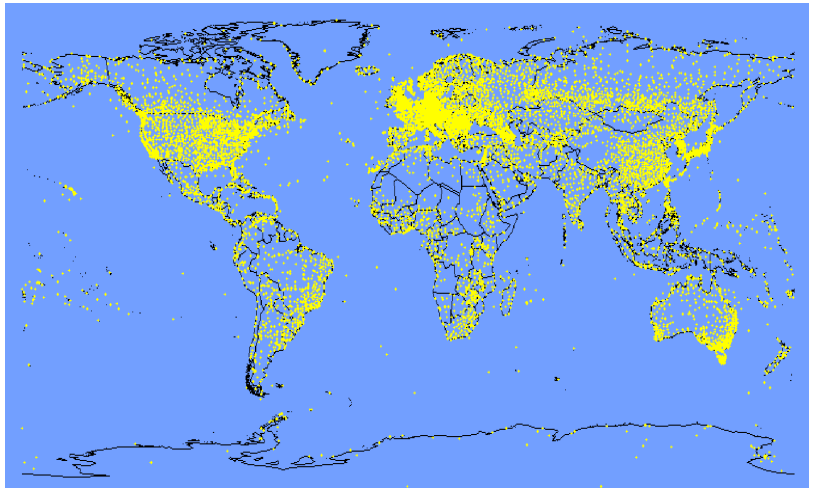

Variations of daily average temperature on the surface of the Earth from 2002 to 2012 (blue line) and its average value (green line) ftp://ftp.ncdc.noaa.gov/pub/data/gsod

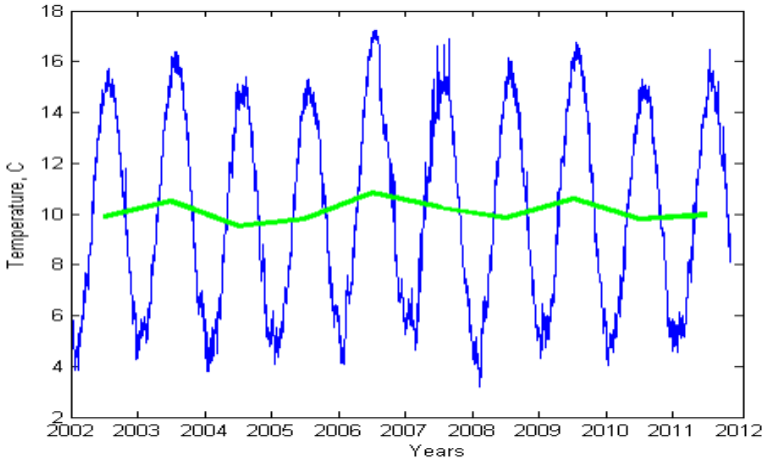

Long-term trends in Sun/Ionosphere parameters

Sun

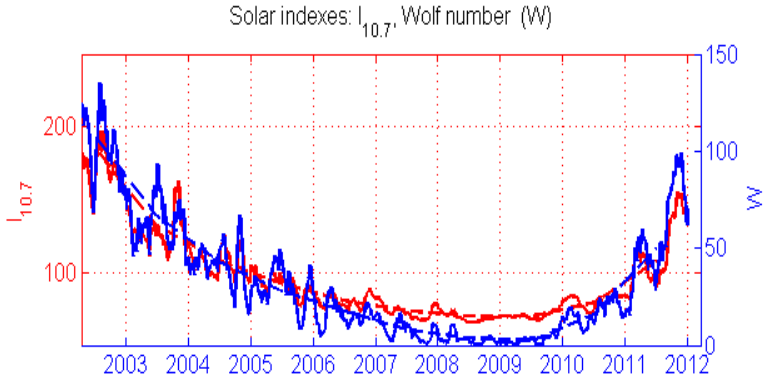

Ionosphere

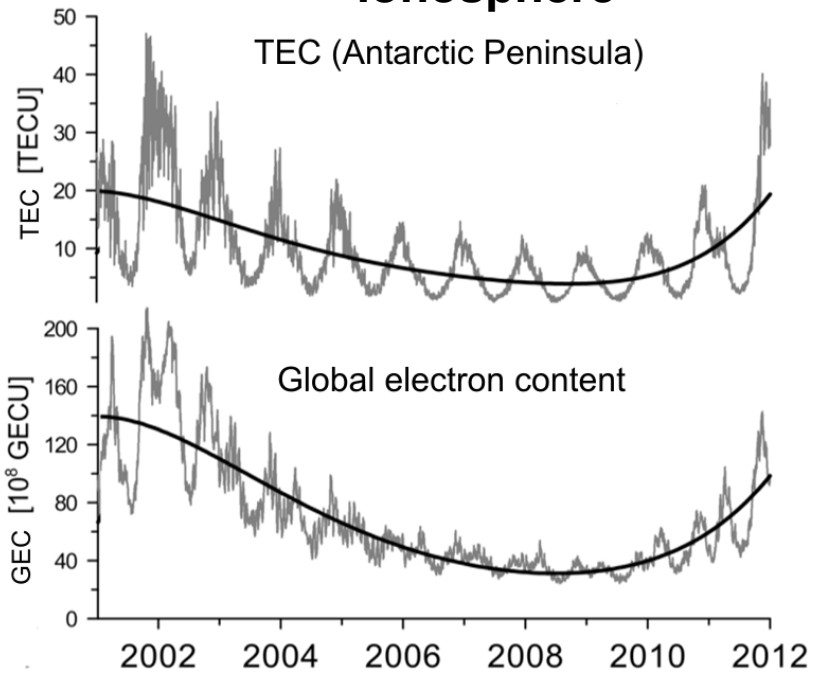

The ways to improve the model

$A_j(t) \equiv \left[\frac{3c}{4\pi^2 a^3 f^{(1)}|z_1|}\right]^2 < |\tilde{M}_j(t)|^2 >$ - electromagnetic activity (j-source), where a - Earth radius, c - speed of light,

$f^{(1)}$ - frequency of first maximum in the point of source

$< |\tilde{M}_j(t)|^2 >$ - mean square of the current moment of j-discharge

$z_1 = \frac{z_0}{\sqrt{2}}\sqrt{1+\sqrt{1+\rho^2}}$ - diagonal element of the impedance

$z_0 = \sqrt{\frac{i\omega\nu_{eff}}{\omega_0^2}}$ - impedance of the isotropic ionosphere

ω_0 - critical frequency of the ionosphere

ω_H - ion gyro frequency

ν_{eff} - electron collision frequency

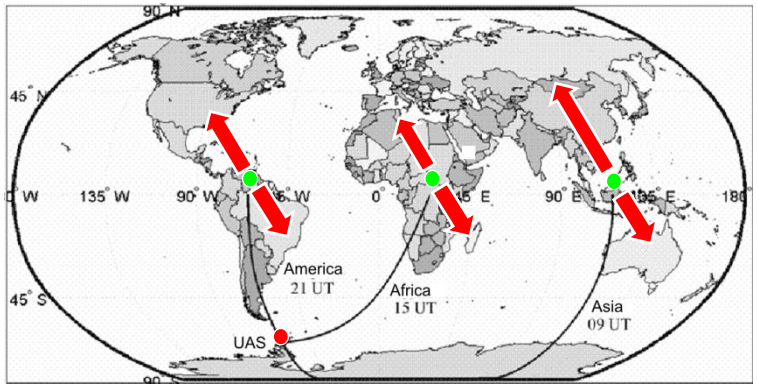

Summary

- The facilities are integrated into single Internet based system which provides remote control of the instruments and transferring of the row data to main server for further processing and visualizing on the web page. This scheme may be effectively used for organizing practical training courses for the students.
- Compact-sized HF and ELF facilities may be used both for studding of the process in the near Earth environment and as educational tools for visualization of these processes and calculation of their characteristics.

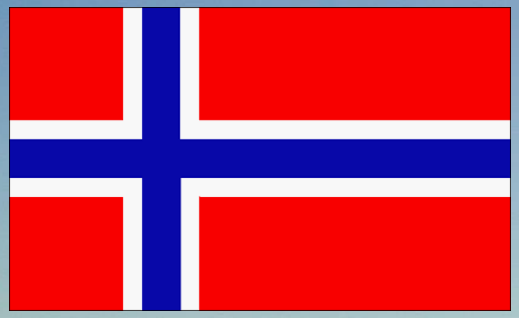

Thank you!